ELSEVIER

Nuclear Physics B 482 [FS] (1996) 497–535

NUCLEAR PHYSICS B [FS]

Meanders: a direct enumeration approach

P. Di Francesco [1], O. Golinelli [2], E. Guitter [3]

Service de Physique Théorique, C.E.A. Saclay, F-91191 Gif sur Yvette, France

Received 1 July 1996; accepted 3 September 1996

Abstract

We study the statistics of semi-meanders, i.e. configurations of a set of roads crossing a river through n bridges, and possibly winding around its source, as a toy model for compact folding of polymers. By analyzing the results of a direct enumeration up to $n = 29$, we perform on the one hand a large-n extrapolation and on the other hand we reformulate the available data into a large-q expansion, where q is a weight attached to each road. We predict a transition at $q = 2$ between a low-q regime with irrelevant winding, and a large-q regime with relevant winding.

PACS: 02.10.Eb; 05.40.+j; 64.60.-i
Keywords: Polymers; Folding; Winding; Meanders; Scaling

1. Introduction

The meander problem is a simply stated combinatorial question: count the number of configurations of a closed non-self-intersecting road crossing an infinite river through a given number of bridges. Despite its apparent simplicity, this problem still awaits a solution, if only for asymptotics when the number of bridges is large. The problem emerged in various contexts ranging from mathematics to computer science [1]. In particular, Arnold re-actualized it in connection with Hilbert's 16th problem, namely the enumeration of ovals of planar algebraic curves [2], and it also appears in the classification of 3-manifolds [3].

[1] E-mail: philippe@spht.saclay.cea.fr
[2] E-mail: golinel@spht.saclay.cea.fr
[3] E-mail: guitter@spht.saclay.cea.fr

PII S0550-3213(96)00505-6

Remarkably, the meander problem can be rephrased in the physical language of critical phenomena, through its equivalence with a particular problem of Self-Avoiding Walks: the counting of the compact foldings of a linear chain.

Several techniques have been applied to this problem: direct combinatorial approaches [4,5], random matrix model techniques [6–8], an algebraic approach using the Temperley–Lieb algebra and Restricted Solid-On-Solid models [9]. Several exact results have been obtain on the way for meander-related issues, including exact sum rules for meandric numbers [7], the solution of the somewhat simpler irreducible meander problem [6,7], and the calculation of a meander-related determinant [9,3].

The present paper is dedicated to a more direct *enumerative* approach and a thorough analysis of its results in the spirit of critical phenomena. The meander problem is generalized to include the case of several non-intersecting but possibly interlocking roads with a weight q per road. The corresponding generating functions are analyzed as functions of q. In particular, we derive their large-q asymptotic expansion in powers of $1/q$.

The paper is organized as follows. In Section 2 we give the basic definitions of meanders and semi-meanders (which correspond to the same problem with a semi-infinite river with a source, around which the roads are free to wind), as well as some associated observables such as the winding. We further give exact solutions to the meander and semi-meander problems at two particular values of q: $q = 1$, where they reduce to a random walk problem, and $q = \infty$, dominated by simple configurations. In Section 3 we explain how to enumerate the semi-meanders for arbitrary number n of bridges, using a fundamental recursive construction. After implementation on a computer, this procedure allowed us to find the semi-meander numbers with up to $n = 29$ bridges. These data are presented and then analyzed by a direct large n extrapolation. On the way we also confirm the scaling hypotheses borrowed from the theory of critical phenomena. Evidence is found for a phase transition for semi-meanders at a value of $q = q_c \simeq 2$ between a low-q and a large-q regimes, discriminated by the relevance of winding around the source. In Section 4 we show how to use the above data to generate a large-q expansion for most of the interesting quantities. This expansion provides an accurate description of the whole $q > q_c$ phase. In Section 5, we analyze the break-down of this expansion, which gives rise to the $q < q_c$ phase. Section 6 briefly describes the small-q expansion of the problem. We gather our conclusions in Section 7. The more technical details are relegated to appendices.

2. The meander problem

2.1. Definitions, observables

A *meander* of order n is a planar configuration of a non-self-intersecting loop (road) crossing a line (river), through a given number $2n$ of points (bridges). We consider as equivalent any two configurations which may be continuously deformed into each

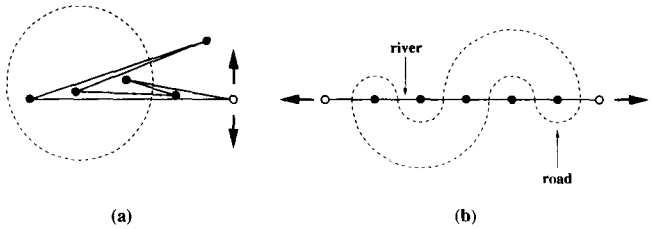

Fig. 1. The mapping between compactly folded closed strip of stamps and meanders. We display a compact folding configuration (a) of a closed strip with $2n = 6$ stamps. To transform it into a meander, first draw a (dotted) line through the centers of the stamps and close it to the left of the picture. Then cut the bottom right hinge (empty circle) and pull its ends apart as indicated by the arrows, so as to form a straight line (b): the straight line forms the river, and the dashed line the road of the resulting meander.

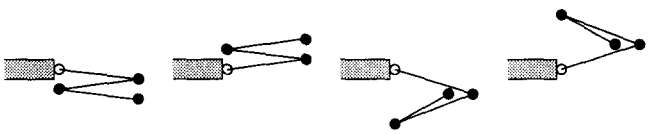

Fig. 2. The 4 inequivalent foldings of a strip of 3 stamps. The fixed stamp is indicated by the empty circle: it is attached to a support (shaded area). The other circles correspond to the edges of the stamps.

other, keeping the river fixed (this is therefore a topological equivalence). The number of inequivalent meanders of order n is denoted by M_n. For instance, we have $M_1 = 1$, $M_2 = 2$, $M_3 = 8, \ldots$ More numbers can be found in [6,7,10].

We stumbled on the meander problem by trying to enumerate the distinct *compact folding* configurations of a closed polymer, i.e. the different ways of folding a closed chain of $2n$ identical constituents onto itself. The best image of such a closed polymer is that of a closed strip of $2n$ identical stamps, attached by their edges, serving as hinges in the folding process: a compactly folded configuration of the strip is simply a folded state in which all the stamps are piled up on top of one of them.

Such a compactly folded configuration is easily identified with a meander configuration as depicted in Fig. 1. Draw a closed line (road) passing though the centers (bridges) of all the piled-up monomers, then open one hinge of the polymer (we choose to always open the bottom right one) and pull the stamps apart so as to form a straight line: the latter is identified with the river, whereas the distorted line becomes the road of the resulting meander.

When the strip of stamps is open (see Fig. 2), we decide to attach the first stamp to a support, preventing the strip from winding around it, while the last stamp has a free extremal edge. In this case, a slightly generalized transformation maps any compactly folded open configuration of $(n - 1)$ stamps to what we will call a *semi-meander* configuration of order n, in the following manner.

As shown in Fig. 3, draw a curve (road) though the $(n - 1)$ centers (bridges) of all the piled-up stamps, then close this curve across the support (this last intersection is the nth bridge), and pull the free edge of the last stamp in order to form a straight half-line (river with a source). The resulting picture is a configuration of a road (the curve) crossing a semi-infinite river (stamps and support) through n bridges: this is

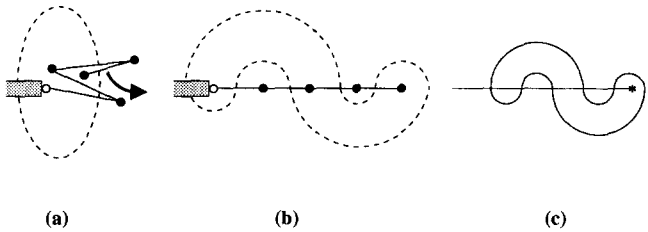

Fig. 3. The mapping of a compactly folded configuration of 4 stamps onto a semi-meander of order 5. (a) draw a (dashed) curve through the pile of stamps and the (shaded) support. (b) pull the free edge of the last stamp to form a half-line (the river with a source). (c) the result is a semi-meander configuration of order 5, namely that of a road, crossing a semi-infinite river through 5 bridges (the source of the river, around which the road is free to wind, is indicated by an asterisk).

called a semi-meander configuration of order n. Note that the road in a semi-meander may wind freely around the source of the river, and that consequently the number of bridges may be indifferently even or odd, as opposed to meanders. The number of distinct semi-meanders of order n is denoted by $\bar{M}_n$. For instance, we have $\bar{M}_1 = 1$, $\bar{M}_2 = 1$, $\bar{M}_3 = 2$, $\bar{M}_4 = 4, \ldots$ More numbers can be found in [4,7] and in Appendix A.

Through its compact folding formulation, the semi-meander problem is a particular reduction of the two-dimensional self-avoiding walk problem, in which only topological constraints are retained. It is therefore natural to define, by analogy with self-avoiding walks the connectivity $\bar{R}$ per stamp and the configuration exponent γ which determine the large-n behavior of the semi-meander numbers as follows:[4]

$$\bar{M}_n \sim \bar{c}\frac{\bar{R}^n}{n^\gamma}. \tag{2.1}$$

The connectivity $\bar{R}$ may be interpreted as the average number of possibilities of adding one stamp to the folded configurations. The exponent γ is characteristic of the (open) boundary condition on the strip of stamps.

A natural observable for self-avoiding walks is the end-to-end distance. The corresponding notion for a compactly folded open strip of stamps is the "distance" between the free end of the strip and, say the support. This distance should also indicate how far the end of the strip is buried inside the folded configuration. It is defined as the minimal length w of a strip of stamps to be attached to the free end, such that a resulting folding with $n-1+w$ stamps has its free end outside of the folding, namely can be connected to the infinity to the right of the folding by a half-line which does not intersect any stamp. Indeed, the infinity to the right can be viewed as the nearest topological neighbor of the support, hence w measures a distance from the free end of the strip to the support. This is illustrated in Fig. 4a, with $n = 5$ and $w = 1$. In the semi-meander formulation (see Fig. 4b), this distance w is simply the *winding* of the road around the source of the river, namely the number of bridges to be added if we continue the river to the right

[4] That the semi-meander numbers $\bar{M}_n$ actually have these leading asymptotics may be proved by deriving upper and lower bounds on $\bar{R}$. See Ref. [7] for further details.

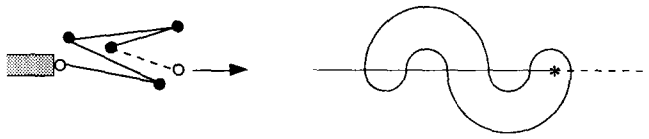

(a) (b)

Fig. 4. The "end-to-end distance" of the folded strip of stamps (a) is the number ($w = 1$ here) of stamps to be added to the strip (the added stamp is represented in dashed line), so that the new free end (empty circle) is in contact with the infinity to the right. This coincides with the "winding" of the corresponding semi-meander (b), namely the number of bridges to be added if we continue the river to the right of its source (dashed line).

of its source. By analogy with self-avoiding walks, we expect the average winding over all the semi-meanders of order n to have the leading behavior

$$\langle w \rangle_n \equiv \frac{1}{\bar{M}_n} \sum_{\text{semi-meanders}} w \sim n^{\nu} , \tag{2.2}$$

where ν is some positive (end-to-end) exponent $0 \leqslant \nu \leqslant 1$, as w is always smaller or equal to n.

In this language, a meander of order n is simply a semi-meander of order $2n$ with winding $w = 0$. By analogy with closed (as compared to open) self-avoiding walks, we expect the asymptotics

$$M_n \sim c \frac{R^{2n}}{n^{\alpha}} , \tag{2.3}$$

where the connectivity per bridge R is the same as that for semi-meanders (2.1), $R = \bar{R}$, and the configuration exponent $\alpha \neq \gamma$ is characteristic of the closed boundary condition on the strip of stamps.

In the following, we will mainly focus our study on the semi-meander numbers.

2.2. *Arches and connected components*

Any semi-meander may be viewed as a particular meander by opening the semi-infinite river as indicated by the arrows on Fig. 5. In the process, the number of bridges is doubled, hence the order is conserved. The resulting meander however is very peculiar. Note that in general a meander is made of an upper (lower) configuration consisting of non-intersecting arches (arcs of road) connecting the bridges by pairs above (below) the river. In the present case the lower configuration is fixed: it is called the rainbow arch configuration of order n (the bridge i is connected to the bridge $(2n - i + 1)$, $i = 1, 2, \ldots, n$). On the other hand, the upper arch configuration may take any of the $\bar{M}_n$ values leading to semi-meanders of order n.

There are however

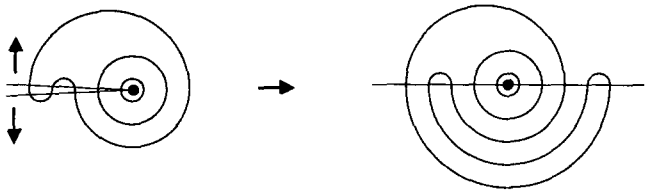

Fig. 5. A semi-meander viewed as a particular meander: the semi-infinite river must be opened up as indicated by the arrows. This doubles the number of bridges in the resulting meander, hence the order is conserved ($n = 5$ here). By construction, the lower arch configuration of the meander is always a rainbow arch configuration of same order.

$$c_n = \frac{(2n)!}{n!(n+1)!} \tag{2.4}$$

distinct arch configurations of order n [7], as is readily proved by recursion ($c_{n+1} = \sum_{0 \leqslant j \leqslant n} c_j c_{n-j}$, with $c_0 = 1$, hence $c_1 = 1$, $c_2 = 2$, $c_3 = 5$, $c_4 = 14, \ldots$: the c_n are called the Catalan numbers). Hence not all upper arch configurations, once supplemented by a lower rainbow arch configuration of same order, lead to an opened semi-meander ($\bar{M}_n < c_n$). This is because, in general, the corresponding object will have $k \geqslant 1$ connected components: we call it a semi-meander of order n with k connected components. Indeed, if the river is folded back into a semi-infinite one, we are simply left with a collection of k possibly interlocking semi-meanders of respective orders $n_1, n_2, \ldots, n_k$, with $n_1 + n_2 + \ldots + n_k = n$. We always have $1 \leqslant k \leqslant n$, and $k = n$ only for the superposition of an upper and a lower rainbow configurations, leading to n concentric circles. We denote by $\bar{M}_n^{(k)}$ the number of inequivalent semi-meanders of order n with k connected components. In particular, we have $\bar{M}_n^{(1)} = \bar{M}_n$ and $\bar{M}_n^{(n)} = 1$ for all n.

The direct numerical study of the asymptotics of the numbers $\bar{M}_n^{(k)}$ turns out to be delicate, as the natural scaling variable of the problem is the ratio $x = k/n$, which depends on n and takes only a discrete set of values. To circumvent this problem, we will study the generating function $\bar{m}_n(q)$ for these numbers, also referred to as the *semi-meander polynomial*,

$$\bar{m}_n(q) = \sum_{k=1}^{n} q^k \bar{M}_n^{(k)} . \tag{2.5}$$

This quantity makes it possible to study the large-n asymptotics of the $\bar{M}_n^{(k)}$ in a global way, by use of extrapolation techniques for all real values of q. The semi-meander polynomial (2.5) may be viewed as the partition function of a statistical assembly of multicomponent semi-meanders of given order n, with a fugacity q per connected component. As such, it is expected to have an extensive large n behavior, namely

$$\bar{m}_n(q) \sim \bar{c}(q) \frac{\bar{R}(q)^n}{n^{\gamma(q)}} , \tag{2.6}$$

where $\bar{R}(q)$ is the partition function per bridge, $\gamma(q)$ is a possibly varying exponent and $\bar{c}(q)$ a function independent of n. For $q \to 0$ ($k = 1$), we must recover the connected semi-meanders, namely that $\bar{m}_n(q)/q \to \bar{M}_n$, i.e.

$$\bar{R}(q) \to R\,, \qquad \gamma(q) \to \gamma\,, \qquad \bar{c}(q)/q \to \bar{c} \tag{2.7}$$

(cf. (2.1)). The notion of winding is well defined for multi-component semi-meanders as well, as the sum of the individual windings of each connected component, namely the *total* number of times the various roads forming the semi-meander wind around the source of the river. Therefore we define

$$\langle w\rangle_n(q) = \frac{1}{\bar{m}_n(q)} \sum_{\substack{\text{multicomp.}\\ \text{semi-meanders}}} w q^k \sim n^{\nu(q)}\,, \tag{2.8}$$

where $\nu(q)$ is the generalized winding exponent for multi-component semi-meanders, satisfying $0 \leqslant \nu(q) \leqslant 1$.

Analogously, we define multi-component meanders of order n, as configurations of k non-intersecting roads ($1 \leqslant k \leqslant n$) crossing the river through a total of $2n$ bridges, and denote by $M_n^{(k)}$ their number. We also define the *meander polynomial*

$$m_n(q) = \sum_{k=1}^{n} q^k\, M_n^{(k)}\,. \tag{2.9}$$

This is nothing but the restriction of (2.5) with $n \to 2n$, to semi-meanders with zero winding $w = 0$. We therefore expect the asymptotics for large n

$$m_n(q) \sim c(q) \frac{R(q)^{2n}}{n^{\alpha(q)}}\,. \tag{2.10}$$

In this estimate, the partition function per bridge $R(q)$ is expected to be identical to that of semi-meanders $\bar{R}(q)$ only if the winding is irrelevant, namely if $\nu(q)$ is strictly less than 1

$$R(q) = \bar{R}(q) \quad \text{iff} \quad \nu(q) < 1\,. \tag{2.11}$$

Otherwise, the fraction of semi-meanders with zero winding may be exponentially small, and we only expect that $R(q) < \bar{R}(q)$ if $\nu(q) = 1$.

2.3. *Exact results for large numbers of connected components ($q = \infty$)*

For very large q, we simply have

$$\bar{m}_n(q) \sim q^n \tag{2.12}$$

as the meander polynomial is dominated by the $k = n$ term, corresponding to the unique semi-meander of order n made of n concentric circular roads, each crossing the semi-infinite river only once. This semi-meander will appear as the rightmost object in the nth line of the tree of Fig. 8. The winding of this semi-meander is clearly $w = n$, hence we have, for $q \to \infty$

$$\bar{R}(q) \to q\,, \qquad \gamma(q) \to 0\,, \qquad \bar{c}(q) \to 1\,, \qquad \nu(q) \to 1\,. \tag{2.13}$$

As to meanders, the only way to build a meander of order n with the maximal number n connected components is that each component be a circle, crossing the river exactly twice. This is readily done by taking any upper arch configuration and completing it by reflection symmetry with respect to the river. This leads to $M_n^{(n)} = c_n$ (cf. (2.4)) meanders with n connected components. By Stirling's formula, we find that when $q \to \infty$ the meander polynomial behaves as

$$m_n(q) \sim c_n q^n \sim \frac{1}{\sqrt{\pi}} \frac{(2\sqrt{q})^{2n}}{n^{3/2}}\,, \tag{2.14}$$

hence, when $q \to \infty$

$$R(q) \to 2\sqrt{q}\,, \qquad \alpha(q) \to 3/2\,, \qquad c(q) \to 1/\sqrt{\pi}\,. \tag{2.15}$$

This confirms the above-mentioned property (2.11) that $R(q) < \bar{R}(q)$ when $\nu(q) = 1$, as $2\sqrt{q} < q$ for large q.

2.4. *Exact results for random walks on a half-line ($q = 1$)*

When $q = 1$ in (2.5), $\bar{m}_n(1)$ simply counts all the multi-component semi-meanders, irrespectively of their number of connected components. This simplifies the problem drastically, as we are simply left with a purely combinatorial problem which can be solved exactly. The multicomponent semi-meanders are obtained by superimposing any arch configuration of order n with the rainbow of order n, hence

$$\bar{m}_n(1) = c_n \sim \frac{1}{\sqrt{\pi}} \frac{4^n}{n^{3/2}} \tag{2.16}$$

by use of Stirling's formula for large n. This gives the values

$$\bar{R}(1) = 4\,, \qquad \gamma(1) = 3/2\,, \qquad \bar{c}(1) = 1/\sqrt{\pi}\,. \tag{2.17}$$

The study of the winding at $q = 1$ is more transparent in the formulation of arch configurations of order n as random walks of $2n$ steps on a semi-infinite line. For each arch configuration of order n, let us label by $1, 2, \ldots, 2n-1$ each segment of river in-between two consecutive bridges, and 0 the leftmost semi-infinite portion, $2n$ the rightmost one. Let $h(i)$, $i = 0, 1, \ldots, 2n$ denote the number of arches passing at the vertical of the corresponding segment i. By definition, $h(0) = h(2n) = 0$. More generally, going along the river from left to right, we have $h(i) = h(i-1) + 1$ (respectively $h(i) = h(i-1) - 1$) if an arch originates from the bridge i (respectively terminates at the bridge i).

The function h satisfies $h(i) \geqslant 0$, for all i, and may be interpreted as a "height" variable, defined on the segments of river, whose graph is nothing but a walk of $2n$ steps as shown in Fig. 6. This may be seen as the two-dimensional extent of a brownian motion of $2n$ steps on a half-line, originating and terminating at the origin of the line.

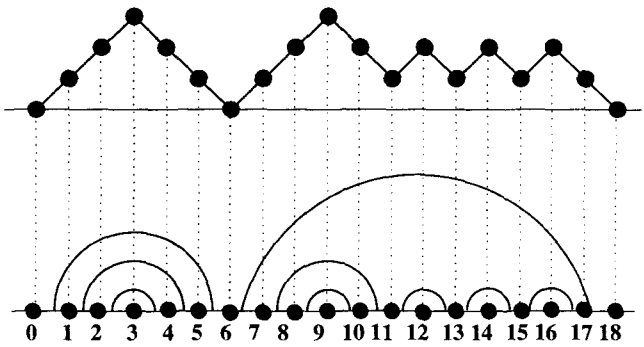

Fig. 6. A walk diagram of 18 steps, and the corresponding arch configuration of order 9. Each dot corresponds to a segment of river. The height on the walk diagram is given by the number of arches intersected by the vertical dotted line.

This interpretation makes the leading behavior $c_n \sim 2^{2n}$ of (2.16) clear: it corresponds to the two possible directions (up or down) that the motion may take at each step. The exponent $3/2$ in (2.16) is characteristic of the boundary condition, namely that the motion is closed and takes place on a half-line (other boundary conditions would lead to different values of γ, e.g. for a closed walk on a line, we would have a behavior $\binom{n}{2n} \sim 2^{2n}/\sqrt{n}$).

In this picture, the winding is simply given by the height $w = h(n)$ of the middle point. Let us evaluate more generally the average height of a point i over the arch configurations of order n. It is given by

$$\langle h(i)\rangle_n = \frac{1}{c_n} \sum_{h \geqslant 0} h A_{n,i}(h) \,, \tag{2.18}$$

where $A_{n,i}(h)$ denotes the number of arch configurations of order n such that $h(i) = h$. A simple calculation [9] shows that

$$A_{n,i}(h) = \left(\binom{i}{\frac{i+h}{2}} - \binom{i}{\frac{i+h}{2}+1} \right) \left(\binom{2n-i}{n-\frac{i-h}{2}} - \binom{2n-i}{n-\frac{i-h}{2}+1} \right) \tag{2.19}$$

as the $A_{n,i}(h)$ walks are simply obtained by gluing two independent walks of i and $2n - i$ steps linking the origin to the height h.

In the case of the winding, $w = h(i = n)$, (2.18) leads to a more compact formula, according to the parity of n

$$\begin{aligned} n = 2p : \quad & \langle w\rangle_{2p} = \frac{\binom{2p}{p}^2}{c_{2p}} - 1 \,, \\ n = 2p+1 : \quad & \langle w\rangle_{2p+1} = 2\frac{\binom{2p}{p}\binom{2p+1}{p}}{c_{2p+1}} - 1 \,. \end{aligned} \tag{2.20}$$

For large n, this gives the following expansion:

$$\langle w\rangle_n = 2\sqrt{\frac{n}{\pi}} - 1 + \frac{5}{4\sqrt{\pi n}} + O(1/n^{3/2}) \tag{2.21}$$

irrespectively of the parity of n. This implies that

$$\nu(q=1) = 1/2\,. \tag{2.22}$$

This is the well-known result for the Brownian motion, for which the extent of the path scales like $n^{1/2}$ for large n. It is instructive to note that, thanks to (2.21), the observable $w+1$ is less sensitive than w to the finite size effects at $q=1$. This will be useful in the forthcoming numerical estimates for arbitrary q where we observe that the numerical extrapolations are improved by considering $w+1$ instead of w. Using (2.19), we may now compute the probability distribution $P_n(w)$ for an arch configuration of order n to have winding $h(n) = w$, which takes for large n the scaling form

$$P_n(w) = \frac{1}{c_n} A_{n,n}(w) \sim \frac{1}{\langle w\rangle_n} f\left(\frac{w}{\langle w\rangle_n}\right) \tag{2.23}$$

with a scaling function f independent of n for large n, readily obtained by use of Stirling's formula, upon writing $w = 2\sqrt{n/\pi}\,\xi$ for large n. This gives

$$f(\xi) = \frac{32}{\pi^2}\xi^2 e^{-(4/\pi)\xi^2} \tag{2.24}$$

for all $\xi > 0$.

For general position $i \neq n$, we find, by a saddle point evaluation of the sum (2.18), that the average profile of arch configurations is a "Wigner" semi-circle

$$\langle h(i)\rangle_n \sim 2\sqrt{\frac{n}{\pi}}\sqrt{x(2-x)} \tag{2.25}$$

when expressed in the scaled position $x = i/n$, $0 \leqslant x \leqslant 2$.

The meanders of order n are the semi-meanders of order $2n$ with winding $w = h(2n) = 0$. They are therefore built as the juxtaposition of two independent walks of length $2n$. Hence

$$m_n(1) = (c_n)^2 \sim \frac{1}{\pi}\frac{4^{2n}}{n^3} \tag{2.26}$$

or, in other words,

$$R(1) = \bar{R}(1) = 4\,, \qquad \alpha(1) = 3\,, \qquad c(1) = 1/\pi\,. \tag{2.27}$$

This is again in agreement with (2.11), as $\nu(1) = 1/2 < 1$, i.e. the winding is irrelevant at $q = 1$.

3. Exact enumeration and its analysis

In this section, we present results of an exact enumeration of $\bar{M}_n^{(k)}$ for small n ($n \leqslant 29$), and analyze their large-n extrapolation. The enumeration is performed by

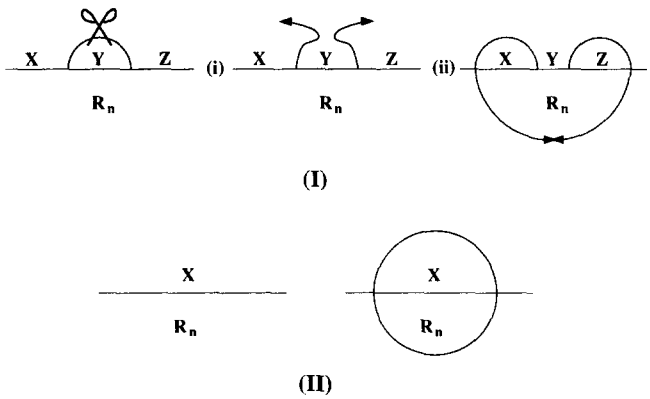

Fig. 7. The construction of all the semi-meanders of order $n+1$ with arbitrary number of connected components from those of order n. Process (I): (i) pick any exterior arch and cut it (ii) pull its edges around the semi-meander and paste them below. The lower part becomes the rainbow configuration $\mathcal{R}_{n+1}$ of order $n+1$. This process preserves the number of connected components $k \to k$. Process (II): draw a circle around the semi-meander of order n. This process adds one connected component $k \to k+1$.

implementing on a computer a recursive algorithm which describes all the semi-meanders up to some given order. Clearly, the complexity is proportional to the Catalan numbers ($c_n \sim 4^n$) hence the limitation on n.

3.1. The main recursion relation

The subsequent numerical study relies on the exploitation of the following recursion relation generating all the semi-meanders of order $(n+1)$ from those of order n.

We start from any semi-meander of order n with k connected components, in the open-river picture. We may construct a semi-meander of order $(n+1)$ in either following way (denoted (I) or (II)), as illustrated in Fig. 7.

(I) Pick any exterior arch, i.e. any arch with no other arch passing above it. Cut it and pull its ends all the way around the others (in order to add two bridges), and reconnect them below, by creating an extra concentric lower arch for the rainbow. In this process, we have $n \to n+1$, but the number of connected components has not changed: $k \to k$. Another way of picturing this transformation is the following: one simply has pulled the exterior arch all the way around the semi-meander and brought it below the figure, creating two new bridges along the way. As no cutting nor pasting is involved, the number of connected components is clearly preserved.

(II) Draw a circle around the semi-meander. This adds a lower concentric semi-circle which increases the order of the rainbow to $(n+1)$, and also adds one connected component to the initial semi-meander $k \to k+1$.

These two possibilities exhaust all the semi-meanders of order $(n+1)$, as the transformation is clearly invertible, by pulling back up the lower external arch of the rainbow. Note that by construction, there are as many possibilities for the process (I) as exterior arches, and the transformation is therefore one-to-many.

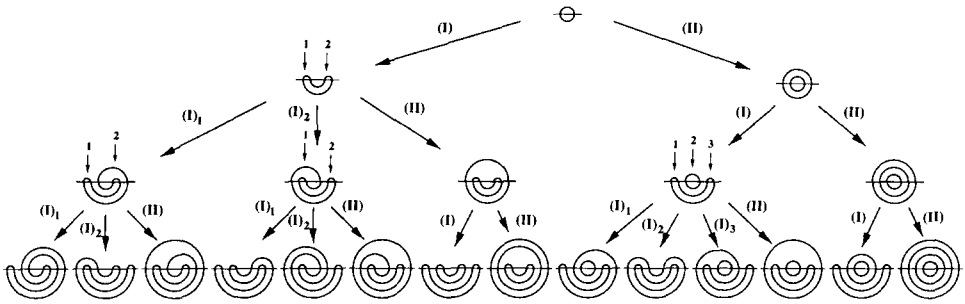

Fig. 8. The tree of semi-meanders down to order $n = 4$. This tree is constructed by repeated applications of the processes (I) and (II) on the semi-meander of order 1 (root). We have indicated by small vertical arrows the multiple choices for the process (I), each of which is indexed by its number. The number of connected components of a given semi-meander is equal to the number of processes (II) in the path going from the root to it, plus one (that of the root).

We may now construct a tree of all the semi-meanders, generated recursively from that of order 1 (root), as displayed in Fig. 8. Note that we have adopted the open-river formulation to represent them.

Keeping track of the connected components, this translates into the following relation between the semi-meander polynomials

$$\bar{m}_{n+1}(q) = \bar{m}_n(q)\langle \text{ext.arch.}\rangle_n(q) + q\bar{m}_n(q)\,, \tag{3.1}$$

where we denoted by $\langle \text{ext.arch.}\rangle_n(q)$ the average number of exterior arches in a semi-meander of order n, weighed by q^k, k its number of connected components. In (3.1), the first term corresponds to all the processes (I), whereas the second term corresponds to (II).

Taking the large-n limit in (3.1), this permits to interpret

$$\bar{R}(q) - q = \langle \text{ext.arch.}\rangle_\infty(q) \tag{3.2}$$

as the limit when $n \to \infty$ of the average number of exterior arches in semi-meanders of order n, weighed by an activity q per connected component.

In particular, when $q \to \infty$, we have

$$\bar{R}(q) - q \to 1 \tag{3.3}$$

as the limiting semi-meander, made of concentric circles, has only one exterior arch. This is a refinement of the large-q estimate in (2.13). When $q = 1$, we find an average of

$$\langle \text{ext.arch.}\rangle_\infty(1) = \bar{R}(1) - 1 = 3 \tag{3.4}$$

exterior arches in arbitrary arch configurations of large order [7]. When $q = 0$, the connected semi-meanders, with $k = 1$, are obtained through repeated action of the process (I) only. This restricts accordingly the tree of Fig. 8. In that case, the partition function per bridge

$$\bar{R} = \bar{R}(0) = \langle \text{ext.arch.}\rangle_\infty(0) \tag{3.5}$$

coincides with the average number of exterior arches in connected semi-meanders, for large n.

3.2. Exact enumeration and large-n extrapolation

In Appendix A, we give an archetypical example of the programs we have implemented to compute the semi-meander numbers and various observables. We have computed the numbers $\bar{M}_n^{(k)}$ for $1 \leqslant k \leqslant n \leqslant 27$, the numbers $\bar{M}_n^{(1)}$ for $n \leqslant 29$. To investigate the winding of semi-meanders, we have also computed the numbers $\bar{M}_n^{(k)}(w)$ of semi-meanders of order n, with k connected components and fixed winding w for $1 \leqslant k \leqslant n \leqslant 24$ (encoding in particular the meander numbers $M_n^{(k)} = \bar{M}_{2n}^{(k)}(0)$), and the semi-meander "profile"

$$\sum_{\substack{\text{semi-meanders} \\ \text{order } n,k \text{ c.c.}}} h(i) \tag{3.6}$$

for all positions $0 \leqslant i \leqslant 2n$. Some of these numbers can be found in Appendix A.

After gathering these numbers into generating functions of q, it is possible to perform large-n extrapolations at fixed q, for the quantities $\bar{R}(q)$, $R(q)$, $\gamma(q)$, $\alpha(q)$, $\bar{c}(q)$, $c(q)$ and $\nu(q)$.

The general extrapolation scheme is the following. Suppose an observed quantity X_n has the following large-n expansion:

$$X_n = \sum_{k=0}^{p} \frac{x_k}{n^k} + O(1/n^{p+1}) . \tag{3.7}$$

Then we get a best estimate of the large-n limit x_0 by iterating p times the difference process $(\Delta f)(n) \equiv f(n+1) - f(n)$ on the function $f(n) = n^p X_n$, with the result

$$\frac{\Delta^p}{p!} n^p X_n = x_0 + O(1/n^{p+1}) . \tag{3.8}$$

This gives perfect results for the Catalan numbers (i.e. $q = 1$) using $X_n = \log(c_{n+1}/c_n)$. This turns out to extend to a whole range of q's in a neighborhood of 1. For instance, $\log \bar{R}(q)$ is extrapolated using $X_n = \log \sqrt{\bar{m}_{n+1}(q)/\bar{m}_{n-1}(q)}$.

The results for $\bar{R}(q)$ and $R(q)$ are displayed in Fig. 9. The two functions are found to coincide in the range $0 \leqslant q \leqslant q_c$ with $q_c \simeq 2$, and to split into $\bar{R}(q) > R(q)$ for $q > q_c$. As explained before, the comparison between $\bar{R}(q)$ and $R(q)$ determines directly whether $\nu(q)$ is 1 or not. The result of Fig. 9 is therefore the signal of a phase transition at $q = q_c$ between a low-q regime where the winding is essentially irrelevant ($\nu(q) < 1$) and a large-q phase with relevant winding ($\nu(q) = 1$).

This is compatible with the direct extrapolation for $\nu(q)$ displayed in Fig. 10, which is however less reliable in the region around $q = 2$, due to its sub-leading (and probably discontinuous) character.

The configuration exponent for semi-meanders $\gamma(q)$ is represented in Fig. 11, for two different orders in the extrapolation scheme (3.8). The extrapolation proves to be

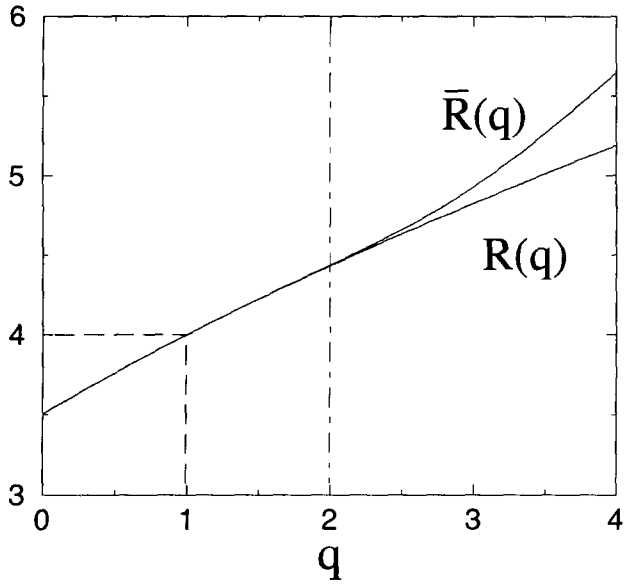

Fig. 9. The functions $\bar{R}(q)$ and $R(q)$ for $0 \leqslant q \leqslant 4$ as results of large-n extrapolations. The two curves coincide for $0 \leqslant q \leqslant 2$ and split for $q > 2$ with $\bar{R}(q) > R(q)$. Apart from the exact value $\bar{R}(1) = R(1) = 4$, we find the estimates $\bar{R}(0) = 3.50(1)$, $\bar{R}(2) = 4.44(1)$, $\bar{R}(3) = 4.93(1)$ and $\bar{R}(4) = 5.65(1)$.

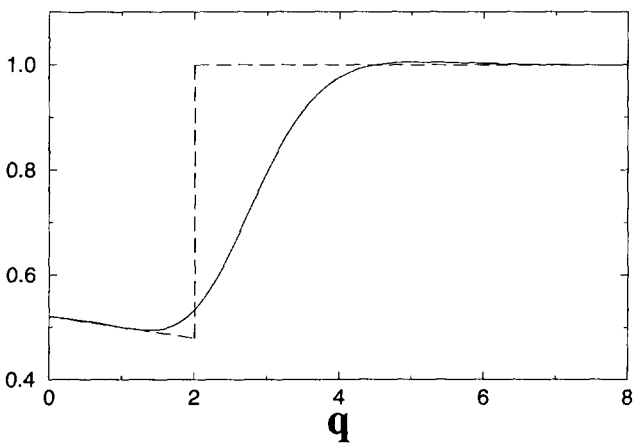

Fig. 10. The winding exponent $\nu(q)$ for $0 \leqslant q \leqslant 8$, as obtained from a large-n extrapolation. We observe a drastic change of behavior between low q's and large q's, with an intermediate regime where the extrapolation fails, hence is not reliable. The dashed line indicates a possible scenario for the exact function $\nu(q)$, compatible with a transition at $q_c \simeq 2$. Apart from the exact value $\nu(1) = 1/2$, we read $\nu(0) = 0.52(1)$.

stable for $0 < q < 2$. For $q > 2$, it develops oscillations around a mean value, estimated to vanish ($\gamma(q) \sim 0$) for q large enough. For simplicity, we chose not to represent the functions $\alpha(q)$, $c(q)$, $\bar{c}(q)$. The coefficient $\bar{c}(q)$ develops a discontinuity at the transition $q = 2$. On the other hand, the functions pertaining to meanders only ($\alpha(q)$ and $c(q)$) do not display any transition at $q = 2$.

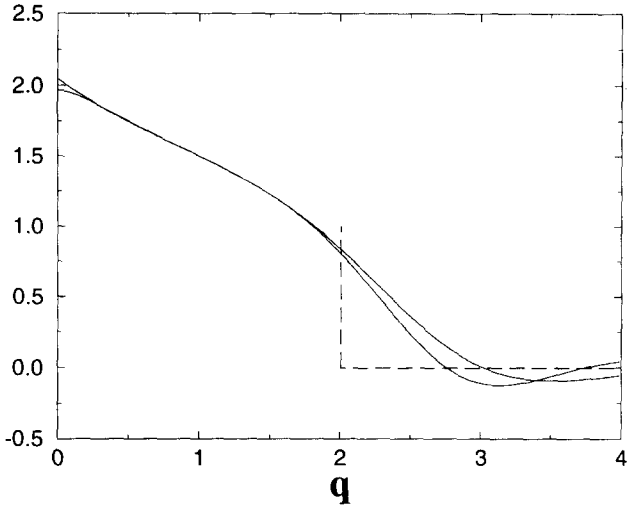

Fig. 11. The configuration exponent $\gamma(q)$ for $0 \leqslant q \leqslant 4$, from two different large-n extrapolations. Apart from the exact value $\gamma(1) = 3/2$, we estimate $\gamma(0) \simeq 2$.

3.3. Scaling functions

By analogy with critical phenomena, in addition to the scaling behaviors (2.6), (2.10) and (2.8) involving the critical exponents $\gamma(q)$, $\alpha(q)$ and $\nu(q)$, we expect to find more refined scaling laws involving scaling functions. A particular example of such scaling functions has been derived for $q = 1$ (2.23), for the probability distribution $P_n(w)$ of the winding w among arch configurations of order n. It involves the scaling function (2.24). For $q = 0$ we expect the same behavior for the corresponding probability distribution

$$P_n^{(0)}(w) = \frac{\bar{M}_n^{(1)}(w)}{\bar{M}_n^{(1)}} \tag{3.9}$$

of winding w among connected semi-meanders of order n. We expect the scaling behavior

$$P_n^{(0)}(w) \sim \frac{1}{\langle w \rangle_n(0)} f^{(0)}\left(\frac{w}{\langle w \rangle_n(0)}\right). \tag{3.10}$$

This is precisely what we observe in Fig. 12, where we plot $\langle w+1 \rangle_n(0)\, P_n^{(0)}(w)$ as a function of the reduced variable $\xi = (w+1)/\langle w+1 \rangle_n(0)$ for different values of n. Indeed, as already explained in the $q = 1$ case, we have taken the variable $(w+1)$ instead of w to improve the convergence. All the data accumulate on a smooth curve, which represents the scaling function $f^{(0)}(\xi)$. The shape of this function is reminiscent of that of the end-to-end distribution for polymers. By analogy, we expect a certain power law behavior for small ξ

$$f^{(0)}(\xi) \sim \xi^{\theta}, \tag{3.11}$$

where θ satisfies the relation

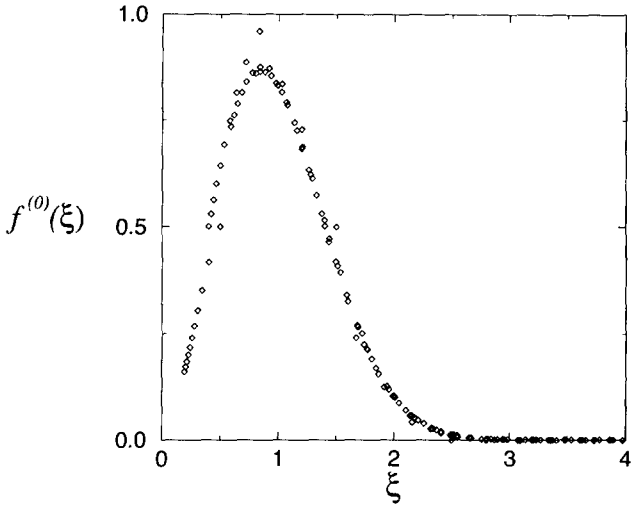

Fig. 12. Plot of $\langle w+1\rangle_n(0)\, P_n^{(0)}(w)$ as a function of the reduced variable $\xi = (w+1)/\langle w+1\rangle_n(0)$ for $n = 2, 3, \ldots, 24$. The points accumulate to a smooth scaling function $f^{(0)}(\xi)$. The erratic points correspond to small values of n, which have not reached the asymptotic regime.

$$\alpha - \gamma = \nu(1+\theta) \tag{3.12}$$

obtained by identifying

$$P_{2n}^{(0)}(0) \propto \frac{1}{n^{\nu}} f^{(0)}\left(\frac{1}{n^{\nu}}\right) \tag{3.13}$$

with

$$\frac{\bar{M}_{2n}^{(1)}(0)}{\bar{M}_{2n}^{(1)}} = \frac{M_n}{\bar{M}_{2n}} \propto n^{\gamma-\alpha}. \tag{3.14}$$

For large ξ, we expect a behavior $f^{(0)}(\xi) \sim \exp(-\text{const.}\,\xi^{\delta})$ with a possible Fisher-law behavior $\delta = 1/(1-\nu)$. The observed function of Fig. 12 is compatible with these limiting behaviors, although we cannot extract reliable estimates of the exponents θ and δ.

As we already did in the case of $q = 1$ (2.25), we can study the average profile of semi-meanders

$$\frac{\langle h(i)\rangle_n(q)}{\sum_{j=0}^{2n}\langle h(j)\rangle_n(q)} \sim \frac{1}{n}\rho(x = i/n; q) \tag{3.15}$$

involving a scaling function $\rho(x; q)$ of the variable x, with $0 \leqslant x \leqslant 2$ for each value of q (with the appropriate normalization such that $\int \rho = 1$). For instance, we have seen in Eq. (2.25) that $\rho(x; 1) = (2/\pi)\sqrt{x(2-x)}$.

We have represented in Fig. 13 these profiles for several values of q. Again, the points accumulate on smooth limiting curves $\rho(x; q)$. We observe a first change of behavior at $q = 1$ between a $q < 1$ regime with a negative cusp at $x = 1$ and a $q > 1$ regime

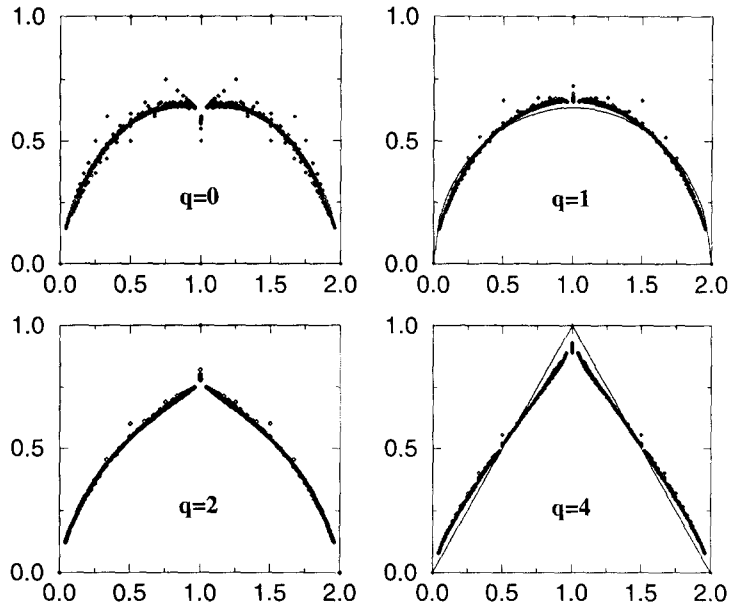

Fig. 13. Semi-meander average profiles for $q = 0, 1, 2, 4$, and $1 \leqslant n \leqslant 24$, as functions of the reduced variable $x = i/n$. For $q = 1$, we also represented the exact large-n Wigner semi-circular limit $\rho(x;1)$. For $q = 4$, we also represented the large-n and q piecewise-linear limit $\rho(x;\infty)$.

with a positive cusp, separated by the Wigner semi-circle, with no cusp at $q = 1$. For large q, $\rho(x;q)$ tends to the limit $\rho(x;\infty) = 1 - |1 - x|$ corresponding to the unique semi-meander made of n concentric circles, which satisfies $h(i) = i$ for $0 \leqslant i \leqslant n$ and $h(i) = 2n - i$ for $n \leqslant i \leqslant 2n$. For small x, we expect a power law behavior of the form

$$\rho(x;q) \sim x^{\varphi(q)}, \tag{3.16}$$

where we identify the exponent $\varphi(q) = \nu(q)$ from $h(1) = 1$ and the fact that $\sum_j h(j) \sim n^{1+\nu(q)}$.

4. Large-q asymptotic expansions

In the previous section, we have observed two regimes for the semi-meander polynomials, namely a low-q regime in which the winding is irrelevant and a large-q regime where the winding is relevant, separated by a transition at a value of $q = q_c \simeq 2$. On the other hand, we have already exhibited an exact solution of the problem at $q = \infty$ (2.13), and a first correction thereof for large q in (3.3). It is therefore tempting to analyze the large-q phase by a systematic expansion in $1/q$. This is performed in the following section, where $\bar{R}(q)$ is expanded up to order 19 in $1/q$, and $\gamma(q)$ is found to vanish identically throughout the large-q regime. In the subsequent section, we compute the large-q expansion of the average winding in semi-meanders, and we find $\nu(q) = 1$ identically in this regime.

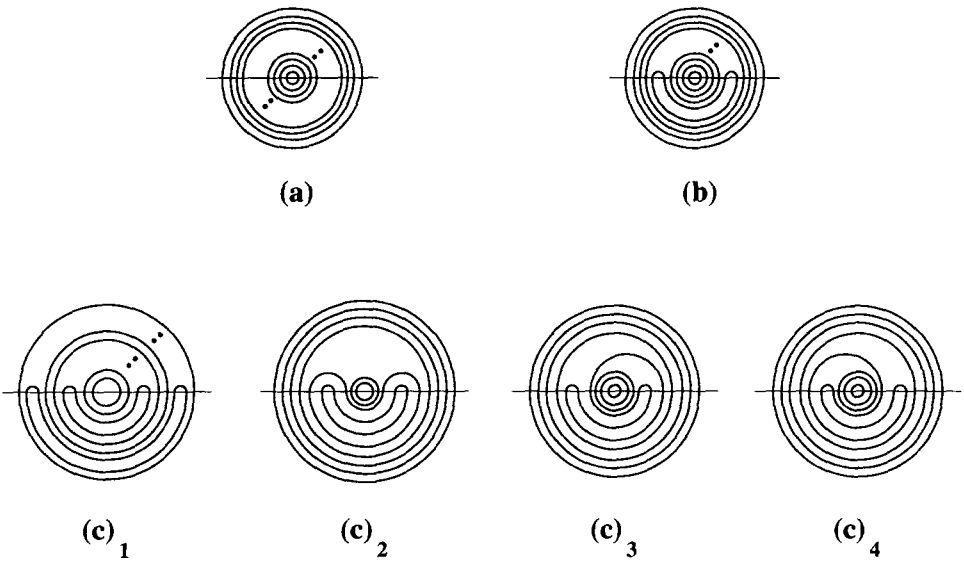

Fig. 14. Semi-meanders with many connected components. (*a*) $k = n$ connected components; there are n circles. (*b*) $k = n - 1$ connected components; there are $(n-2)$ circles and one "kidney". (*c*) $k = n - 2$ connected components; there are respectively $(c)_1$ two disjoint kidneys and $(n-4)$ circles; $(c)_2$ two kidneys included in one another and $(n-4)$ circles; $(c)_3$ and $(c)_4$ one "spiral" and $(n-3)$ circles.

4.1. Large-q asymptotic expansion of the semi-meander polynomial

In this section we derive the large-q expansion of the semi-meander polynomial $\bar{m}_n(q)$ of Eq. (2.5) as

$$\bar{m}_n(q) = q^n \left(\bar{M}_n^{(n)} + \frac{\bar{M}_n^{(n-1)}}{q} + \frac{\bar{M}_n^{(n-2)}}{q^2} + \dots \right) \tag{4.1}$$

involving the semi-meander numbers in the form $\bar{M}_n^{(n-k)}$, $k = 0, 1, 2, \dots$ Remarkably, these numbers, for arbitrary $n \geqslant 2k-1$, are polynomials of n, which furthermore exhibit some special structure allowing for an explicit large-q expansion of $\bar{R}(q)$.

The section is organized as follows. We first derive the polynomial form of the $\bar{M}_n^{(n-k)}$, valid for $n \geqslant 2k-1$, together with the corrections to be added for smaller n's.

The re-exponentiation of $\bar{m}_n(q)$ in the form (2.6) induces strong constraints on the polynomials $\bar{M}_n^{(n-k)}$, which allow for their complete determination up to $k = 18$, out of their first values for small n, which were enumerated exactly up to $n = 27$.

For starters, let us first compute the numbers $\bar{M}_n^{(n-k)}$ for $k = 0, 1, 2$.

As we already mentioned, the leading term $\bar{M}_n^{(n)} = 1$ in the expansion (4.1) counts the unique semi-meander of order n with n connected components made of concentric circles only, and which we refer to as the leading semi-meander (cf. Fig. 14a). This yields the first polynomial

$$p_0(n) = \bar{M}_n^{(n)} = 1 \tag{4.2}$$

for all $n \geqslant 0$.

The sub-leading term is made of the

$$p_1(n) = \bar{M}_n^{(n-1)} = n - 1 \tag{4.3}$$

"kidney"-type perturbations of the leading semi-meander, displayed in Fig. 14b.

The next-to-leading term consists of the semi-meanders of order n with $(n-2)$ connected components, which may be obtained as follows.

(i) A first possibility consists in taking two "kidney"-type perturbations of the leading semi-meander (see Figs. 14c_1 and c_2), which are either
  (i1) (Fig. 14c_1) disjoint, hence a total of $(n-2)(n-3)/2$ choices for the positions of two kidneys.
  (i2) (Fig. 14c_2) included in one another, hence a total of $(n-3)$ choices for the position of the double kidney, or 0 choice if $n = 2$.

(ii) The second possibility is a larger "spiral"-type perturbation of the leading semi-meander, with a total of $(n-2)$ available positions, and there are two such perturbations (see Figs. 14c_3 and c_4).

Summing up all these contributions gives[5]

$$\begin{aligned}\bar{M}_n^{(n-2)} &= \frac{(n-2)(n-3)}{2} + (n-3) + \delta_{n,2} + 2(n-2) \\ &= \frac{n^2+n-8}{2} + \delta_{n,2}\,,\end{aligned} \tag{4.4}$$

hence a polynomial

$$p_2(n) = \frac{n^2+n-8}{2}\,. \tag{4.5}$$

We see here the first appearance of a correction for small n, in that an extra boundary term $(\delta_{n,2})$ has to be added at $n = 2$, to recover the fact that $\bar{M}_2^{(0)} = 0$.

More generally, let us consider the number $\bar{M}_n^{(n-k)}$ for large n and finite k. The corresponding semi-meanders are obtained in the tree of Fig. 8 by applying to the root k times the process (I) and $(n-1-k)$ times the process (II). This gives $\binom{n-1}{k} \sim n^k/k!$ possible choices ($k \ll n$). These choices however are not completely independent.

Recall that the process (I) may be applied to any exterior arch of the semi-meander. In the situation where $k \ll n$, the semi-meander will most probably have only one exterior arch (generated by the last process, most probably of the type (II)), and there will be only one choice for (I), creating a kidney. If two or more processes (I) are applied *consecutively*, the number of exterior arches may grow, and yield more semi-meanders (e.g. the application of two consecutive processes (I) yields three possibilities: two included kidneys, or any of the two spirals). Such an effect is however sub-leading, as the number of choices of two or more consecutive processes (I) grows at most like

[5] Throughout this section, we use the fact that $\bar{M}_n^{(0)} = \delta_{n,0}$, i.e. there are no semi-meanders with zero connected component, except for the vacuous semi-meander of order 0.

n^{k-1}. Collecting all these extra combinatorial factors permits, like in (4.4), to write the number $\bar{M}_n^{(n-k)} = p_k(n)$ as a polynomial of degree k in n for large enough n, and fixed k, with moreover a leading term $n^k/k!$.

For smaller n, the above consecutive choices are affected by the boundaries of the tree. Recall for instance that the double included kidneys of Fig. $14c_2$, obtained by two successive applications of (I) on two concentric circles, may only exist for $n \geqslant 4$. We have therefore needed to specify that their number (generically equal to $(n-3)$) vanishes for $n = 3$ (granted) and $n = 2$, the latter resulting in a boundary correction $\delta_{n,2}$. More generally, expressing that the combinatorial expressions found are only valid for large enough n's will translate into boundary terms, studied in detail in Appendix B. We simply quote the result here, valid for all $n \geqslant k$,

$$\bar{M}_n^{(n-k)} = p_k(n) + \sum_{j=0}^{k-2} \bar{\mu}_j^{(k)} \delta_{n,2k-2-j}\,, \tag{4.6}$$

where the $\bar{\mu}_j^{(k)}$ are some positive integers. In particular, (4.6) shows that the formula $\bar{M}_n^{(n-k)}$ is a pure polynomial $p_k(n)$ with no corrections as soon as $n \geqslant 2k-1$. This property is derived in Appendix B, where the first correction $\mu_0^{(k)} = c_{k-1}$ is also obtained.

The precise determination of the p_k's and the $\mu_j^{(k)}$ could be in principle achieved directly by pursuing the above method used for $k = 0, 1, 2$. However, the complexity of this program is comparable to that of the exact enumeration of the semi-meander numbers. Instead we can guess the coefficients of $p_k(n)$ by matching our data for $\bar{M}_n^{(n-k)}$ with the form (4.6). This can be pushed further by exploiting the re-exponentiation property of $\bar{m}_n(q)$, which implies relations between the coefficients of the $p_k(n)$, as discussed now.

The property (4.6) must be reconciled with the large-n behavior of $\bar{m}_n(q)$ (2.6), namely that for n sufficiently large

$$\log \bar{m}_n(q) = n \log \bar{R}(q) - \gamma(q) \log n + \log \bar{c}(q) + o(1)\,. \tag{4.7}$$

Such an expansion is valid for all q, and we can in particular study it for large q. On the other hand, up to any order k in the $1/q$ expansion, and by choosing $n \geqslant 2k-1$, we may also write

$$\begin{aligned} \log \frac{\bar{m}_n(q)}{q^n} &= \log\left(1 + \frac{p_1(n)}{q} + \frac{p_2(n)}{q^2} + \ldots + \frac{p_k(n)}{q^k} + O\left(\frac{1}{q^{k+1}}\right)\right) \\ &= \sum_{m=1}^{k} \frac{1}{q^m} \sum_{j=1}^{m} \frac{(-1)^{j-1}}{j} \sum_{\substack{k_1+\ldots+k_j=m \\ k_i \geqslant 1}} p_{k_1}(n) p_{k_2}(n) \ldots p_{k_j}(n) + O\left(\frac{1}{q^{k+1}}\right)\,. \end{aligned} \tag{4.8}$$

In this expansion, the coefficient of $1/q^m$ is a polynomial of n, as a sum of products of polynomials of n. Comparing this with an expansion of (4.7) in $1/q$, we see that its degree is at most 1. Therefore, there exist two sequences of coefficients (α_k, β_k), such that

$$p_k(n) = \alpha_k n + \beta_k + \sum_{j=2}^{k} \frac{(-1)^j}{j} \sum_{\substack{k_1+\ldots+k_j=k \\ k_i \geqslant 1}} p_{k_1}(n) p_{k_2}(n) \ldots p_{k_j}(n) \tag{4.9}$$

with the correspondence

$$\log \bar{R}(q) = \log q + \sum_{k\geqslant 1} \frac{\alpha_k}{q^k},$$

$$\log \bar{c}(q) = \sum_{k\geqslant 1} \frac{\beta_k}{q^k}. \tag{4.10}$$

Moreover, there can be no $\log n$ term in the expansion of (4.7), hence the remarkable result

$$\gamma(q) = 0. \tag{4.11}$$

This result is expected to hold as long as the corrections to the polynomial behavior of the $\tilde{M}_n^{(n-k)}$ are negligible. As we will see, this condition defines precisely the large-q phase $q > q_c$. Therefore the exponent $\gamma(q)$ vanishes identically over the whole phase $q > q_c$. In view of, say, the exact value $\gamma(q=1) = 3/2$, this property cannot persist in the small $q < q_c$ phase. This is not surprising since the first correction $\mu_0^{(k)} = c_{k-1}$ (for $k = n/2 + 1$) implies an additional power law correction of the form $1/n^{3/2}$.

For $n \geqslant 2k-1$, (4.9) is a quasi-recursion relation for the polynomials p_k, hence for the semi-meander numbers $\tilde{M}_n^{(n-k)}$. This relation is exploited in Appendix C to generate from our numerical data the polynomials $p_k(x)$ for $0 \leqslant k \leqslant 18$, together with their corrections. Using these polynomials, it is now straightforward to read the functions $\bar{R}(q)$ and $\bar{c}(q)$ using (4.10), with the result

$$\begin{aligned}
\bar{R}(q) &= q + 1 + \frac{2}{q} + \frac{2}{q^2} + \frac{2}{q^3} - \frac{4}{q^5} - \frac{8}{q^6} - \frac{12}{q^7} - \frac{10}{q^8} - \frac{4}{q^9} + \frac{12}{q^{10}} + \frac{46}{q^{11}} \\
&\quad + \frac{98}{q^{12}} + \frac{154}{q^{13}} + \frac{124}{q^{14}} + \frac{10}{q^{15}} - \frac{102}{q^{16}} + \frac{20}{q^{17}} - \frac{64}{q^{18}} + O\left(\frac{1}{q^{19}}\right), \\
\bar{c}(q) &= 1 - \frac{1}{q} - \frac{4}{q^2} - \frac{4}{q^3} + \frac{14}{q^5} + \frac{44}{q^6} + \frac{56}{q^7} + \frac{28}{q^8} - \frac{82}{q^9} - \frac{252}{q^{10}} - \frac{388}{q^{11}} \\
&\quad - \frac{588}{q^{12}} - \frac{772}{q^{13}} - \frac{620}{q^{14}} + \frac{1494}{q^{15}} + \frac{5788}{q^{16}} + \frac{7580}{q^{17}} - \frac{690}{q^{18}} + O\left(\frac{1}{q^{19}}\right).
\end{aligned} \tag{4.12}$$

It is interesting to compare the result of these large-q expansions to the previous direct large-n extrapolations of Section 3. As far as $\bar{R}(q)$ is concerned, we find a perfect agreement for the values $q \geqslant 2$, down to $q = 2$, where we find $\bar{R}(2) \simeq 4.442(1)$ using (4.12), in perfect agreement with the previous estimate. The precision of (4.12) increases with q, leading to far better estimates than before: $\bar{R}(3) \simeq 4.92908(1)$, $\bar{R}(4) \simeq 5.6495213(1)\ldots$

As to $\gamma(q)$, our prediction that $\gamma(q) = 0$ for all $q > 2$ is compatible with the previous extrapolation of Fig. 11, where this value is represented in dashed line. We therefore

expect $\gamma(q)$ to have a discontinuity at $q = 2$, where it goes from a non-zero $\gamma(q = 2^-)$ value to zero. This will be confirmed by the forthcoming analysis of the low-q phase in Section 5.

4.2. *Large-q asymptotic expansion of the semi-meander winding*

In this section we first examine the contribution of the circles to the winding of semi-meanders in the large-q phase. It turns out to be of the order n throughout this phase, implying that the winding exponent $\nu(q) = 1$ for all $q > q_c$. In a second step, we compute the large-q expansion of the average winding by techniques similar to those of the previous section, showing that the circles contribute only for a finite fraction of the winding in the large-q phase. This study will single out the value $q_c = 2$ with a very good precision.

To enumerate the total number of circles in order n semi-meanders, we simply have to count the semi-meanders with a marked circle, in one-to-one correspondence with pairs of semi-meanders of total order $(n-1)$ (since the marked circle separates the original meander into two disconnected pieces, its inside and outside). Hence, the average number of circles in semi-meanders is given by

$$\langle \text{circ.} \rangle_n(q) = q \frac{\sum_{j=0}^{n-1} \bar{m}_j(q)\, \bar{m}_{n-1-j}(q)}{\bar{m}_n(q)} \tag{4.13}$$

valid for all q and n, with the convention that $\bar{m}_0(q) = 1$. Using the large-n asymptotics $\bar{m}_n(q) \sim \bar{c}(q)\bar{R}(q)^n$, with $\gamma(q) = 0$ throughout the large-q regime, we find

$$\langle \text{circ.} \rangle_n(q) \sim nq \frac{\bar{c}(q)}{\bar{R}(q)} . \tag{4.14}$$

The average number of circles therefore grows like n which in turn implies that

$$\nu(q) = 1 , \qquad q > q_c \tag{4.15}$$

throughout the large-q regime, since each circle contributes 1 to the winding and clearly $\langle w \rangle \geqslant \langle \text{circ.} \rangle$. Note that the above argument relies crucially on the fact that $\gamma(q) = 0$, and thus cannot be applied to the small q regime. Indeed, for $q = 1$, (4.13) simply gives $\langle \text{circ.} \rangle_n(q = 1) = 1$ for all n, hence a very different behavior.

The quantity $\sigma(q) = \lim_{n\to\infty} \langle \text{circ.} \rangle_n(q)/n$ is simply given by the Taylor expansion of $q\bar{c}(q)/\bar{R}(q)$,

$$\sigma(q) = 1 - \frac{2}{q} - \frac{4}{q^2} + \frac{2}{q^3} + \frac{8}{q^4} + \frac{14}{q^5} + \frac{22}{q^6} - \frac{14}{q^7} - \frac{66}{q^8} - \frac{98}{q^9} - \frac{54}{q^{10}} + \frac{106}{q^{11}} + \frac{20}{q^{12}} - \frac{282}{q^{13}} - \frac{220}{q^{14}} + \frac{1602}{q^{15}} + \frac{3428}{q^{16}} - \frac{1330}{q^{17}} - \frac{13824}{q^{18}} + O\left(\frac{1}{q^{19}}\right) . \tag{4.16}$$

Let us now turn to the large-q expansion of the average winding of semi-meanders (2.2). This requires a refined study of the semi-meander numbers $\bar{M}_n^{(n-k)}(w)$ with fixed

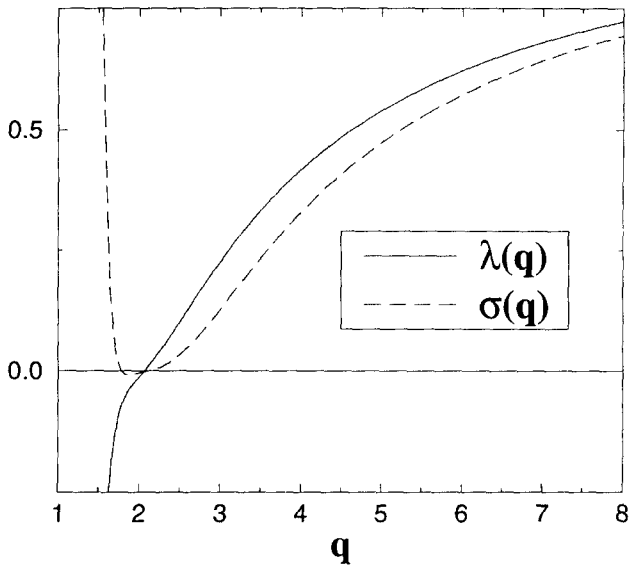

Fig. 15. The series $\lambda(q)$ (4.18) and $\sigma(q)$ (4.16) of $1/q$ up to order 14 and 18 respectively, for $1 < q < 8$. Both curves seem to vanish at $q = 2$.

winding w, which display a similar polynomial structure as the $\bar{M}_n^{(n-k)}$. The study of the corresponding generating function is presented in Appendix D and leads to

$$\langle w \rangle_n(q) = \lambda(q) n + \mu(q) , \tag{4.17}$$

where the coefficients $\lambda(q)$ and $\mu(q)$ have the following large-q expansions up to order 14 in $1/q$:

$$\begin{aligned}
\lambda(q) &= 1 - \frac{2}{q} - \frac{2}{q^2} + \frac{2}{q^3} + \frac{2}{q^4} + \frac{2}{q^5} + \frac{10}{q^6} - \frac{6}{q^7} - \frac{14}{q^8} - \frac{10}{q^9} \\
&\quad + \frac{22}{q^{10}} + \frac{86}{q^{11}} - \frac{58}{q^{12}} - \frac{222}{q^{13}} - \frac{118}{q^{14}} + O\left(\frac{1}{q^{15}}\right) , \\
\mu(q) &= \frac{2}{q} + \frac{10}{q^2} + \frac{22}{q^3} + \frac{54}{q^4} + \frac{134}{q^5} + \frac{246}{q^6} + \frac{622}{q^7} + \frac{1434}{q^8} + \frac{3178}{q^9} \\
&\quad + \frac{6834}{q^{10}} + \frac{13786}{q^{11}} + \frac{30834}{q^{12}} + \frac{66590}{q^{13}} + \frac{140582}{q^{14}} + O\left(\frac{1}{q^{15}}\right) .
\end{aligned} \tag{4.18}$$

It can be checked directly that $\lambda(q) > \sigma(q)$ hence the circles only contribute for a finite fraction of the total winding. The plots of the functions $\lambda(q)$ and $\sigma(q)$ are displayed in Fig. 15. Remarkably, both coefficients seem to vanish at the same point $q = 2$ with an excellent precision. Since these coefficients must be positive, we deduce that our large-q formulas break down for $q < 2$. We interpret this as yet another evidence of the drastic change of behavior of the average winding $\langle w \rangle$, which is no longer linear in n below q_c, and we find $q_c = 2$ with an excellent precision.

The actual break-down of the large-q phase is studied more systematically in next section.

5. The break-down of the large-q expansion for $q < q_c$

The properties of the large-q phase are intimately based on the polynomial structure of the numbers $\bar{M}_n^{(n-k)}$. In this section, we explain the break-down of this phase by the precise structure of the non-polynomial corrections (4.6) to this behavior. The phase transition occurs when these corrections become dominant. The detailed analysis of these corrections shows a strong resemblance between the low q phase and a meander (zero-winding) regime.

The corrections to the polynomial behavior of the $\bar{M}_n^{(n-k)}$ are gathered in the function

$$\bar{\mu}_n(q) = \sum_{k=0}^{n} \left(\bar{M}_n^{(n-k)} - p_k(n)\right) q^{n-k} = \sum_{k=\lfloor (n+2)/2 \rfloor}^{n} \bar{\mu}_{2k-2-n}^{(k)} q^{n-k}. \tag{5.1}$$

The numbers $\bar{\mu}_{2k-2-n}^{(k)}$ are listed for $n/2 < k < n = 2, 3, \ldots, 9$ in Appendix C. With the only difference that we are now dealing with rational fractions of n instead of polynomials, we can carry the same large-n expansion as in Section 4.1, to extract the large-n asymptotics of $\bar{\mu}_n(q)$, with the result, according to the parity of n,

$$\begin{aligned} \bar{\mu}_{2n}(q) &\sim \bar{c}_+(q) \frac{\bar{R}_1(q)^{2n}}{(2n)^{\gamma_1(q)}}, \\ \bar{\mu}_{2n-1}(q) &\sim \bar{c}_-(q) \frac{\bar{R}_1(q)^{2n-1}}{(2n-1)^{\gamma_1(q)}}. \end{aligned} \tag{5.2}$$

Using the results of Appendix C, we get the following large-q expansions (incorporating the large n asymptotics of $c_n \sim 4^n/(\sqrt{\pi} n^{3/2})$)

$$\begin{aligned} \bar{R}_1(q) &= 2\sqrt{q}\left(1 + \frac{1}{q} + \frac{3}{2q^2} - \frac{3}{2q^3} - \frac{29}{8q^4} + O\left(\frac{1}{q^5}\right)\right), \\ \bar{c}_+(q) &= \frac{2}{q}\sqrt{\frac{2}{\pi}}\left(1 + \frac{23}{q} + \frac{283}{q^2} + \frac{3027}{q^3} + \frac{313751}{q^4} + O\left(\frac{1}{q^5}\right)\right), \\ \bar{c}_-(q) &= \frac{2}{q}\sqrt{\frac{2}{\pi q}}\left(3 + \frac{40}{q} + \frac{417}{q^2} + \frac{4418}{q^3} + \frac{44991}{q^4} + O\left(\frac{1}{q^5}\right)\right). \end{aligned} \tag{5.3}$$

Due to the rational fractions of n we have dealt with, we cannot conclude that $\gamma_1(q) = 3/2$ (the $3/2$ comes from the Catalan number asymptotics) identically for large q. We expect this to hold only in the $q \to \infty$ limit, whereas for finite q, $\gamma_1(q)$ is some function of q.

We can now write

$$\bar{m}_n(q) \simeq \bar{c}_0(q)\, \bar{R}_0(q)^n + \bar{c}_\pm(q) \frac{\bar{R}_1(q)^n}{n^{\gamma_1(q)}} + \ldots, \tag{5.4}$$

where $\pm$ is chosen according to the parity of n and we have indexed by 0 the functions $\bar{R}(q)$ and $\bar{c}(q)$ corresponding to the polynomial contributions to the $\bar{M}_n^{(n-k)}$, with the asymptotic expansions (4.12). When q is large, the first term dominates as $\bar{R}_0(q) \sim q$, whereas $\bar{R}_1(q) \sim 2\sqrt{q}$. This justifies a posteriori the identification $\bar{R}(q) = \bar{R}_0(q)$ in the large-q regime of Section 4. The properties derived in Section 4 for the large-q regime will however break down if $\bar{R}_1(q) \geqslant \bar{R}_0(q)$, i.e. when the corrections become dominant. We expect such a crossing of phases to take place at the transition point $q = q_c$, at which $\bar{R}_1(q_c) = \bar{R}_0(q_c)$. In this scenario, $\bar{R}(q) = \bar{R}_1(q)$ for all $q < q_c$, and the exponent $\gamma(q)$ jumps abruptly from its large $q > q_c$ value $\gamma_0(q) = 0$, to a non-zero value $\gamma_1(q_c) \neq 0$. This mechanism explains the jump in the value of $\gamma(q)$ at the vicinity of $q = q_c$, as observed in Fig. 11. In this figure, we have represented in dashed line the purported value $\gamma(q) = 0$ for $q > 2$, which must be substituted to the (bad) large-n estimate in this regime, whereas we still rely on the (good) $q < 2$ estimate.

To reconcile this scenario with the picture described in Section 3, in which for $q < q_c$ the winding of semi-meanders becomes irrelevant (i.e. $\bar{R}(q) = R(q)$), we should have $\bar{R}_1(q) = R(q)$ below the transition point q_c, where the semi-meanders enter their meander-like phase. Since the meanders themselves do not display any transition at $q = q_c$, it is tempting to infer that $\bar{R}_1(q) = R(q)$ for all values q. As we will see now, this is corroborated by the large-q expansion (5.3) for $\bar{R}_1(q)$, which turns out to coincide with that of $R(q)$ for meanders (2.10). The latter is easily carried out for the meander numbers, whose structure, given in Appendix E, is very similar to that of the semi-meander corrections. More precisely, the meander numbers $M_n^{(n-k)}$ take the general form

$$M_n^{(n-k)} = c_n r_k(n) , \tag{5.5}$$

where $r_k(x)$ is a rational fraction of x, with total degree k. With the values listed in Appendix E, we find the following large-q expansion for the functions $R(q)$ and $c(q)$ of (2.10), up to order 6 in $1/q$

$$\begin{aligned} R(q) &= 2\sqrt{q}\left(1 + \frac{1}{q} + \frac{3}{2q^2} - \frac{3}{2q^3} - \frac{29}{8q^4} - \frac{81}{8q^5} - \frac{89}{16q^6} + O\left(\frac{1}{q^7}\right)\right) , \\ c(q) &= \frac{1}{\sqrt{\pi}}\left(1 - \frac{6}{q} - \frac{28}{q^2} + \frac{92}{q^3} + \frac{196}{q^4} + \frac{224}{q^5} - \frac{2412}{q^6} + O\left(\frac{1}{q^7}\right)\right) . \end{aligned} \tag{5.6}$$

The exponent $\alpha(q)$ is also found to tend to the Catalan value $3/2$ when q tends to infinity, but appears to be a non-constant function of q for all finite q. Remarkably, the first terms of the large-q series expansions of $R(q)$ and those of the correction to semi-meanders $\bar{R}_1(q)$ coincide!

In conclusion, all our results conspire to suggest that the semi-meanders undergo at $q = q_c$ a transition from a "meander"-like regime $q < q_c$, governed by the meander partition function per bridge $R(q) \equiv \bar{R}_1(q)$, to another regime $q > q_c$, governed by $\bar{R}_0(q)$. The order parameter for this transition is clearly

$$\lim_{n\to\infty} \frac{1}{n}\langle w\rangle_n = \begin{cases} \lambda(q) & \text{for } q > q_c \\ 0 & \text{for } q < q_c \end{cases} \tag{5.7}$$

which vanishes for $q < q_c$ (irrelevant winding, i.e. $\nu(q) < 1$) and is non-zero for $q > q_c$ (relevant winding, i.e. $\nu(q) = 1$). With the order parameter (5.7), the transition is found to be continuous, as the leading coefficient $\lambda(q)$ (4.18) vanishes at $q = q_c$. The smooth character of the transition is also visible from the fact that $\bar{R}(q)$ and $R(q)$ approach each other tangentially at $q = q_c$, and that the coefficient $\bar{c}_0(q) = \bar{R}(q)\sigma(q)/q$ of the large-q dominant contribution to $\bar{m}_n(q)$ vanishes at $q = q_c$ (see Fig. 15).

6. Small q behavior of the semi-meander polynomial

The very existence of asymptotics of the form (2.6) for the semi-meander numbers, with a smooth enough function $\bar{R}(q)$ has highly non-trivial consequences on the numbers $\bar{M}_n^{(k)}$. We have already seen how the numbers $\bar{M}_n^{(n-k)}$, for large n and finite k, are linked to each other (4.8) in order for (2.6) to hold for large q. Let us now examine its consequences on the small q and large-n behavior of $\bar{m}_n(q)$. Let us expand $\bar{m}_n(q)$ around $q = 0$ up to order k, and take the large-n asymptotics of each term in the expansion:

$$\begin{aligned} \bar{m}_n(q) &= \sum_{j=1}^{k} \bar{M}_n^{(j)} q^j + O(q^{k+1}) \\ &\sim \bar{c}(q)\ \frac{\bar{R}(q)^n}{n^{\gamma(q)}} \\ &= \frac{\bar{c}q}{n^{\gamma(q)}} R(0)^n \left(1 + q\frac{\bar{R}'(0)}{\bar{R}(0)} + O(q^2)\right)^n \\ &= \bar{c}\, q \frac{\bar{R}(0)^n}{n^{\gamma}} \sum_{j=1}^{k} \frac{n^{j-1}}{(j-1)!} \left(q\frac{\bar{R}'(0)}{\bar{R}(0)}\right)^{j-1} + O(q^{k+1}), \end{aligned} \tag{6.1}$$

where we have only retained the leading n asymptotics in each q^j term, and used the $q \to 0$ limits (2.7) (actually, we have assumed that $q \sim 1/n$). Comparing with the $\bar{M}_n$ asymptotics (2.1), we finally get

$$\frac{\bar{M}_n^{(k)}}{\bar{M}_n^{(1)}} \sim \frac{1}{(k-1)!} \left(n\frac{\bar{R}'(0)}{\bar{R}(0)}\right)^{k-1}, \tag{6.2}$$

valid for large n and finite k. This is actually very similar to the behavior of the $\bar{M}_n^{(n-k)} \sim n^k/k!$ for large n and finite k, and may be deduced from the main recursion relation for semi-meanders as well. Indeed, the number $\bar{M}_n^{(k)}$ of semi-meanders of order n with k connected components is obtained from that of order 1 (root) by $(k-1)$ applications of the process (II) (see Fig. 8), and $(n-k)$ applications of the process (I), whereas the $\bar{M}_n^{(1)}$ connected semi-meanders are obtained through the process (I)

only. Apart from the relative combinatorial factor $\binom{k-1}{n-1} \sim n^{k-1}/(k-1)!$ accounting for the $(k-1)$ choices of process (II) among the total of $(n-1)$ steps, we must consider that whenever a step (II) is chosen instead of a step (I), some freedom in the overall choice is lost. Eq. (6.2) tells us that this corresponds to an average factor of $\bar{R}'(0)/\bar{R}(0)$ per step (II) taken instead of a step (I). We checked (6.2) numerically, by performing a large-n extrapolation of the appropriate ratio for a few values of k. We find a very good agreement with the estimate

$$\frac{\bar{R}'(0)}{\bar{R}(0)} \sim 0.154(1)\,. \tag{6.3}$$

7. Conclusion

In this paper, we have analyzed the meander problem in the language of critical phenomena, by analogy with Self-Avoiding Walks. In particular, we have displayed various scaling behaviors, involving both scaling exponents and scaling functions. We have presented strong evidence for the existence of a phase transition for semi-meanders weighed by a factor q per connected component (road). In a large-q regime ($q > q_c$), the winding is found to be relevant, with a winding exponent $\nu(q) = 1$, while the configuration exponent $\gamma(q) = 0$. Throughout this phase, a finite fraction $\sigma(q)/\lambda(q)$ of the winding is due to circles, i.e. circular roads with only one bridge, winding around the source of the river. In this regime, the partition function per bridge for semi-meanders $\bar{R}(q)$ is strictly larger than that of meanders $R(q)$. The particular form of its large-q series expansion in $1/q$ (4.12) with slowly alternating integer coefficients, which furthermore grow very slowly with the order, and its purported re-summation (D.14), suggest a possible re-expression in terms of modular forms of q, yet to be found. In a low-q regime $q < q_c$, $\bar{R}(q)$ and $R(q)$ coincide, in agreement with an irrelevant winding $\nu(q) < 1$. The exponent $\gamma(q)$ is no longer 0, but a strictly positive function of q.

We have estimated the value of the transition point $q_c \simeq 2$ with an excellent precision, and we conjecture that $q_c = 2$ exactly. This special value of q has already been singled out in the algebraic study of the meander problem, in connection with the Temperley-Lieb algebra [9]. There, we have been able to re-express the meander and semi-meander partition functions as that of some Restricted Solid-On-Solid model, whose Boltzmann weights are positive precisely iff $q \geqslant 2$, indicating very different behaviors for $q < 2$ and $q > 2$.

In the large-q phase, in addition to the exact values $\nu(q) = 1$ and $\gamma(q) = 0$, we can use the asymptotic expansion (4.12) to get $\bar{R}(q)$ with a very good precision. The somewhat sub-leading meander quantities $R(q)$ and $\alpha(q)$ are more difficult to evaluate in this regime.

A number of questions remain unsettled. There still remains to find the varying exponents $\gamma(q)$ and $\nu(q)$ in the $q < 2$ regime, as well as the precise value of $R(q) = \bar{R}(q)$. Although we improved our numerical estimates, we are limited to conjectures.

For $q = 0$, we confirm a previous conjecture [7] that $\gamma = 2$, and that [6] $\alpha = 7/2$. We also conclude from the numerical analysis that $\nu(0) \simeq 0.52(1)$ is definitely not equal to the trivial random-walk exponent $1/2$. For $q = 2$, we have an amusing guess for $R(2) = \bar{R}(2) = \pi\sqrt{2} = \Gamma(1/4)\Gamma(3/4) = 4.442\ldots$ inspired from possible infinite product formulas for $\bar{R}(q)$.

Acknowledgements

We thank M. Bauer for a critical reading of the manuscript.

Appendix A. Algorithm for the enumeration of semi-meanders

The following is a simple computer algorithm directly inspired by the recursion relation of Section 3.1.

There, it has been shown that one can construct a *tree* of all the semi-meanders generated recursively with processes (I) and (II), as displayed in Fig. 8. Each *node* at *depth* n represents a semi-meander of order n. To have a finite cost of computation, the order is limited to *nmax* and the nodes of depth *nmax* appear to be *leaves*. The algorithm we used consists in visiting all the leaves from left to right, following the branches, as a (clever) squirrel.

To do that, the rules are

(a) The squirrel starts at the root (upper node).

(b) When the squirrel is on a intermediate node (not a leaf), it follows the leftmost branch which it has not yet visited and the depth increases by 1. If all the branches of a given node have been visited, the squirrel goes back up one level and the depth decreases by 1.

(c) When the squirrel is on a leaf (depth *nmax*), it goes back up one level and the depth becomes $(nmax - 1)$.

The reader can convince himself that the above rules describe a systematic and complete visit of the tree. Of course, when the squirrel is on a node, it can measure a lot of interesting quantities like the number of connected components, the winding number... These measures are added up and analyzed at the end of the enumeration.

From a Fortran point of view, many representations of (semi-)meanders are possible. In the open-river formulation, each semi-meander is made of a lower rainbow arch configuration (which we need not code) and an upper arch configuration of order n. For convenience, we label the $2n$ bridges of the river from $i = -n + 1$ to $i = n$, and the system of arches is described by a sequence of integers $\{A(i); i = -n + 1, \ldots, n\}$, where $A(i) \in \{-n + 1, \ldots, n\}$ is the label of the bridge connected with the bridge i. The following Fortran program enumerates the connected semi-meanders. For simplicity, only the process (I) is coded and the number of connected components is always $k = 1$. The arch to be broken $(j, A(j))$ begins at the bridge j and ends at the bridge $A(j)$.

The process (I) splits this arch into two arches $(-n, j)$ and $(A(j), n+1)$. When the squirrel climbs back up one level, the two extremal arches $(-n+1, A(-n+1))$ and $(A(n), n)$ are re-sealed to give one arch $(A(-n+1), A(n))$. At this stage, we know that the next arch to break starts at bridge $j = A(n) + 1$. This ensures the completeness of the algorithm.

```
      PARAMETER (nmax = 14)                          ! maximal order
      INTEGER A(-nmax+1:nmax)                        ! arch representation
      INTEGER Sm(nmax)                               ! semi-meander counter
      INTEGER n                                      ! current depth (or order)
      INTEGER j                                      ! next branch to visit
      DATA n, Sm/0, nmax*0/                          ! n and Sm initialized to 0
      A(0) = 1                                       ! single-arch semi-meander
      A(1) = 0
    2 n = n + 1                                      ! a new node is visited
      Sm(n) = Sm(n) + 1
      j = -n + 1                                     ! leftmost (exterior) arch
    1 IF((n.EQ.nmax).OR.(j.EQ.n+1)) GOTO 3           ! up or down?
      A(A(j)) = n+1                                  ! go down with process (I)
      A(n+1) = A(j)
      A(j) = -n
      A(-n) = j
      GOTO 2
    3 A(A(-n+1)) = A(n)                              ! going up
      A(A(n)) = A(-n+1)
      j = A(n)+1                                     ! next arch to break
      n = n - 1
      IF (n .GT. 1) GOTO 1
      PRINT '(i3, i15)', (n, Sm(n), n = 1, nmax)
      END
```

It is possible to use the left–right symmetry to divide the work by two. It is also possible to adapt the program for a parallel computer. For that, an intermediate size ($n1 = 11$, for instance) is chosen. A first (little) run is made with $nmax = n1$, which gives $\bar{M}(n1)$ leaves. In a second (big and parallelized) run, each of these leaves is now taken as the root of a (sub-)tree and treated independently of the others. At the end, all the results of the sub-trees are collected. The calculations of this article have be done on the parallel Cray-T3D (128 processors) of the CEA-Grenoble, with approximately 7500 hours × processors.

We have computed $\bar{M}_n$ (the (pure) semi-meander number of order n) up to $n = 29$, $\bar{M}_n^{(k)}$ (semi-meander number of order n with k connected components) up to $n = 27$ and the other quantities up to $n = 24$. The reader can obtain an electronic copy of the numerical data upon request from the authors. We content ourselves with giving, in Table A.1, the $\bar{M}_n$ and our last row ($n = 27$) of the $\bar{M}_n^{(k)}$.

Table A.1
The numbers $\bar{M}_n^{(k)}$ of semi-meanders of order n with k connected components, obtained by exact enumeration on the computer: on the left, the one-component semi-meander numbers ($k = 1$) are given for $n \leqslant 29$; on the right, n is fixed to 27 and $1 \leqslant k \leqslant n$. The $\bar{M}_n^{(k)}$ for $n < 27$ can be obtained by request from the authors

n	$\bar{M}_n$	n	$\bar{M}_n$	k	$\bar{M}_{27}^{(k)}$	k	$\bar{M}_{27}^{(k)}$
1	1	16	1053874	1	369192702554	16	2376167414
2	1	17	3328188	2	2266436498400	17	628492938
3	2	18	10274466	3	6454265995454	18	153966062
4	4	19	32786630	4	11409453277272	19	34735627
5	10	20	102511418	5	14161346139866	20	7159268
6	24	21	329903058	6	13266154255196	21	1333214
7	66	22	1042277722	7	9870806627980	22	220892
8	174	23	3377919260	8	6074897248976	23	31851
9	504	24	10765024432	9	3199508682588	24	3866
10	1406	25	35095839848	10	1483533803900	25	374
11	4210	26	112670468128	11	619231827340	26	26
12	12198	27	369192702554	12	236416286832	27	1
13	37378	28	1192724674590	13	83407238044		
14	111278	29	3925446804750	14	27346198448		
15	346846			15	8352021621		

Appendix B. Correction terms for semi-meanders with large number of connected components

In this appendix, we show that the corrections to the polynomial expression (4.6) for the numbers $\bar{M}_n^{(n-k)}$ occur only for $n \leqslant 2k-2$, and derive the first correction $\mu_0^{(k)}$ of (4.6) for $n = 2k-2$. The result reads

$$\mu_0^{(k)} = c_{k-1}\,, \tag{B.1}$$

where the c_n are the Catalan numbers (2.4).

As explained in Section 4, the polynomial part of $\bar{M}_n^{(n-k)}$ is generically obtained as a sum of combinatorial factors, counting all the possible occurrences of perturbations of the leading semi-meander (order n, n components) which have the same order n, but have only $n-k$ connected components. A perturbation, by definition, is made of a core, which does not contain any circle, supplemented by circles. The core is generically made of p irreducible semi-meanders with a total order n_0, and a total of (n_0-k) connected components. By irreducible, we mean that no circle can separate the semi-meander in two disconnected pieces. This core is completed by $(n-n_0)$ circles, to form a semi-meander of order n. Enumerating all perturbations of the leading meander with $n-k$ components amounts to enumerating all the ways of completing cores by circles. There are exactly

$$\binom{n-n_0+p}{p} = \frac{(n-n_0+p)(n-n_0+p-1)\ldots(n-n_0+1)}{p!} \tag{B.2}$$

possible decorations of the above core by circles. The polynomial form (B.2) of the

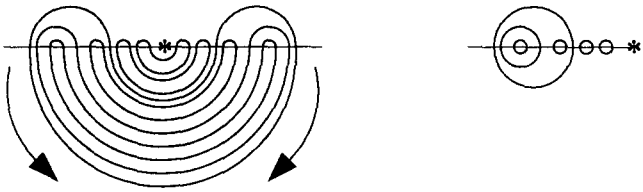

Fig. B.1. Arbitrarily disjoint or included kidneys are equivalent to symmetric meanders upon folding back the river, as indicated by the arrows. The latter are in one-to-one correspondence with arch configurations of the same order.

combinatorial factor is however only valid for $n \geqslant n_0 - p$. When $n \leqslant n_0 - p - 1$, we have to add a correction to the polynomial form to get a vanishing result, equal to $(-1)^{p+1}$ for the largest $n = n_0 - p - 1$. The largest n at which such corrections occur is obtained by maximizing $n_0 - p$. As the core does not contain any circle, each of its $n_0 - k$ connected components is at least of order 2, hence

$$n_0 \geqslant 2(n_0 - k) \quad \Rightarrow \quad n_0 \leqslant 2k . \tag{B.3}$$

This inequality is saturated for a core made of k kidneys. Minimizing p consists in taking $(k-1)$ arbitrary kidneys included in one, for which $p = 1$. We therefore find that the first correction to the polynomial behavior (4.6) occurs at $n = 2k - 2$.

There are exactly c_{k-1} possible choices of these $(k-1)$ kidneys, in one-to-one correspondence with arch configurations of order $(k-1)$ as illustrated in Fig. B.1, upon a folding procedure. Each corresponding core contributes 1 to the correction $\mu_0^{(k)}$, which completes the proof of (B.1).

More generally, we expect corrections to the polynomial part of $\bar{M}_n^{(n-k)}$ for all $k \leqslant n \leqslant 2k-2$, hence the form (4.6). In Appendix C, the structure of the first 9 successive corrections is found, together with the polynomial part of $\bar{M}_n^{(n-k)}$, up to $k = 18$.

Appendix C. Fine structure of the semi-meander numbers

As shown in Appendix B, the polynomial part in (4.6) of the semi-meander numbers $p_k(n)$ is equal to the semi-meander number $\bar{M}_n^{(n-k)}$ for $n \geqslant 2k-1$. In addition, the polynomials p_k are subject to the quasi-recursion relation (4.9), which leaves only two coefficients of p_k to be fixed, once the p_l, $l \leqslant k-1$ are known (we have $p_0(n) = 1$). It is therefore straightforward to derive the first 13 polynomials p_k from our numerical data, as only the two values $p_k(2k-1) = \bar{M}_{2k-1}^{(k-1)}$ and $p_k(2k) = \bar{M}_{2k}^{(k)}$ are required, and the corresponding numbers are known up to $k = 13$.

However, knowing the p_k's up to $k = 13$, we get a list of all the corrections

$$\mu_j^{(k)} = \bar{M}_{2k-2-j}^{(k-2-j)} - p_k(2k-2-j) \tag{C.1}$$

to these polynomials needed to get the correct values of $\bar{M}_n^{(n-k)}$, up to $k = 13$. The resulting table of corrections displays a remarkable structure (very close to that of

meander numbers, studied in Appendix E), which reads as follows, according to the parity of j:

$$\bar{\mu}_{2j}^{(p+1+j)} = c_p \frac{2^j}{j!} \frac{(2p+1)!}{(2p+3j)!} \Pi_{4j-1}(n) \quad \text{with } n = 2p\,,$$
$$\bar{\mu}_{2j+1}^{(p+1+j)} = c_p 3 \frac{2^j}{j!} \frac{(2p)!}{(2p+3j)!} \Pi_{4j}(n) \quad \text{with } n = 2p-1\,, \tag{C.2}$$

valid for all $j \geqslant 0$, where c_p are the Catalan numbers (2.4), and the $\Pi_k(n)$ are monic polynomials of degree k.

Proceeding in parallel (determining the p_k and the corrections simultaneously), we can proceed further up to $k = 18$, with the result

$$p_0(x) = 1\,,$$
$$p_1(x) = x - 1\,,$$
$$p_2(x) = (x^2 + x - 8)/2\,,$$
$$p_3(x) = (x^3 + 6x^2 - 31x - 24)/3!\,,$$
$$p_4(x) = (x^4 + 14x^3 - 49x^2 - 254x)/4!\,,$$
$$p_5(x) = (x^5 + 25x^4 - 15x^3 - 1105x^2 - 1066x + 1680)/5!\,,$$
$$p_6(x) = (x^6 + 39x^5 + 145x^4 - 2895x^3 - 10226x^2 + 8616x + 31680)/6!\,,$$
$$p_7(x) = (x^7 + 56x^6 + 532x^5 - 5110x^4 - 50141x^3 - 20146x^2 + 377208x + 282240)/7!\,,$$
$$p_8(x) = (x^8 + 76x^7 + 1274x^6 - 5264x^5 - 165991x^4 - 422156x^3 + 1979116x^2 + 6031824x + 1128960)/8!\,,$$
$$p_9(x) = (x^9 + 99x^8 + 2526x^7 + 2646x^6 - 413511x^5 - 2570589x^4 + 4826744x^3 + 55185444x^2 + 54007920x - 29756160)/9!\,,$$
$$p_{10}(x) = (x^{10} + 125x^9 + 4470x^8 + 30090x^7 - 803607x^6 - 10282755x^5 - 6206320x^4 + 302065660x^3 + 838000656x^2 - 179320320x - 914457600)/10!\,,$$
$$p_{11}(x) = (x^{11} + 154x^{10} + 7315x^9 + 96360x^8 - 1170477x^7 - 31531038x^6 - 116748115x^5 + 1085347340x^4 + 7183991276x^3 + 4813856784x^2 - 20917209600x - 15487718400)/11!\,,$$
$$p_{12}(x) = (x^{12} + 186x^{11} + 11297x^{10} + 231330x^9 - 921657x^8 - 78859242x^7 - 632084629x^6 + 2301195270x^5 + 41279402956x^4 + 93554770056x^3 - 181951879968x^2 - 528315782400x - 281652940800)/12!\,,$$

$$
\begin{aligned}
p_{13}(x) = (&x^{13} + 221x^{12} + 16679x^{11} + 478621x^{10} + 1380093x^9 - 164767317x^8 \\
&-2382680443x^7 - 496896257x^6 + 172979664286x^5 + 862378655996x^4 \\
&-433580004936x^3 - 7916932037664x^2 - 9843473134080x \\
&-4807260057600)/13!\,, \\
p_{14}(x) = (&x^{14} + 259x^{13} + 23751x^{12} + 899171x^{11} + 8661653x^{10} \\
&-285047763x^9 - 7202313547x^8 - 30034731727x^7 + 538444152246x^6 \\
&+5357996127484x^5 + 6470339335096x^4 - 67697579511744x^3 \\
&-1914708540384000x^2 - 156970678394880x - 54050540544000)/14!\,, \\
p_{15}(x) = (&x^{15} + 300x^{14} + 32830x^{13} + 1575210x^{12} + 26278252x^{11} \\
&-378408030x^{10} - 18419182210x^9 - 164903537370x^8 \\
&+1145711810243x^7 + 25071998561610x^6 + 89293562501780x^5 \\
&-342807873156840x^4 - 2342105695034496x^3 - 3394586375786880x^2 \\
&-1602031548902400x + 1953665505792000)/15!\,, \\
p_{16}(x) = (&x^{16} + 344x^{15} + 44260x^{14} + 2614640x^{13} + 63321622x^{12} \\
&-244465312x^{11} - 40783574260x^{10} - 621949980080x^9 \\
&+743774155553x^8 + 92574072382792x^7 + 650521234967240x^6 \\
&-658128229828160x^5 - 19409328228712176x^4 \\
&-53224642530877824x^3 - 35515613029674240x^2 \\
&+48894886046361600x + 121101107871744000)/16!\,, \\
p_{17}(x) = (&x^{17} + 391x^{16} + 58412x^{15} + 4155820x^{14} + 134381702x^{13} \\
&+605876362x^{12} - 78440970036x^{11} - 1905575960860x^{10} \\
&-7182404321807x^9 + 271696014206903x^8 + 3438145428617536x^7 \\
&+5440767496706360x^6 - 113308202712264496x^5 \\
&-594837570662080656x^4 - 742844861844630912x^3 \\
&+780842535860839680x^2 + 4213612687918233600x \\
&+2696110704967680000)/17!\,, \\
p_{18}(x) = (&x^{18} + 441x^{17} + 75684x^{16} + 6372756x^{15} + 261854502x^{14} \\
&+3203791542x^{13} - 128136377252x^{12} - 5023361538468x^{11} \\
&-45509495478447x^{10} + 602361827803593x^9 + 14435051961445752x^8 \\
&+67015410007677768x^7 - 451434378729887216x^6 \\
&-4879430147272561776x^5 - 11678841781394909184x^4 \\
&+60418030640092669 44x^3 + 780987501567660441 60x^2 \\
&+148841653993843507200x - 44176378569523200 00)/18!\,. \qquad \text{(C.3)}
\end{aligned}
$$

The first Π's read

$$
\begin{aligned}
\Pi_3(x) &= x^3 + \frac{33}{2}x^2 + \frac{49}{2}x + 12\,,\\
\Pi_7(x) &= x^7 + 44x^6 + \frac{1397}{2}x^5 + 3371x^4 + \frac{13229}{2}x^3 + 11735x^2 + 6336x + 1440\,,\\
\Pi_{11}(x) &= x^{11} + \frac{163}{2}x^{10} + 2814x^9 + \frac{198453}{4}x^8 + 405471x^7 + 1586409x^6\\
&\quad + 4522625x^5 + \frac{53075437}{4}x^4 + 13577913x^3 + 14321997x^2 + 3974616x\,,\\
\Pi_{15}(x) &= x^{15} + 129x^{14} + 7462x^{13} + 248370x^{12} + \frac{9911591}{2}x^{11} + \frac{11187899}{2}x^{10}\\
&\quad + 345882086x^9 + 1392155925x^8 + \frac{12479885017}{2}x^7 + \frac{44260908189}{2}x^6\\
&\quad + 30440330807x^5 + 71900294130x^4 + 17319985020x^3\\
&\quad - 28987682544x^2 - 36059230080x - 10059033600\,,\\
\Pi_0(x) &= 1\,,\\
\Pi_4(x) &= x^4 + \frac{47}{3}x^3 + 31x^2 + \frac{37}{3}x + 20\,,\\
\Pi_8(x) &= x^8 + \frac{124}{3}x^7 + \frac{1283}{2}x^6 + \frac{18479}{6}x^5 + \frac{8543}{2}x^4 + \frac{72077}{6}x^3\\
&\quad + 26106x^2 - 4994x - 840\,,\\
\Pi_{12}(x) &= x^{12} + 77x^{11} + \frac{5135}{2}x^{10} + \frac{88129}{2}x^9 + 341193x^8 + 1023192x^7\\
&\quad + \frac{5147959}{2}x^6 + \frac{35955101}{2}x^5 + 23942231x^4 - 16806044x^3\\
&\quad + 18500028x^2 - 21290040x - 6350400\,,\\
\Pi_{16}(x) &= x^{16} + \frac{368}{3}x^{15} + 6845x^{14} + \frac{664235}{3}x^{13} + \frac{8557681}{2}x^{12} + \frac{135562460}{3}x^{11}\\
&\quad + \frac{452366205}{2}x^{10} + \frac{1940546440}{3}x^9 + \frac{11216097197}{2}x^8 + \frac{89505296956}{3}x^7\\
&\quad + \frac{9305821085}{2}x^6 + \frac{27505324345}{3}x^5 + 164921583110x^4\\
&\quad - 422241984828x^3 - 328334271840x^2\\
&\quad - 252250683840x - 40475635200\,.
\end{aligned}
\tag{C.4}
$$

Appendix D. Semi-meanders and winding

In this appendix, we study the numbers $\bar{M}_n^{(k)}(w)$ of semi-meanders of order n, with k connected components and winding w. The winding w has the same parity as the order n, hence we consider the following generating function:

$$\tilde{m}_n(q,t) = \sum_{k=0}^{n-1} q^{n-k} \sum_{j=0}^{\min(k,\lfloor n/2 \rfloor)} t^j \bar{M}_n^{(n-k)}(n-2j) \tag{D.1}$$

interpreted as the partition function for semi-meanders weighed by q per connected component and $1/\sqrt{t}$ per winding unit (up to a global normalization factor). In the large-q limit we now repeat the analysis performed in Section 4.1, by Taylor-expanding $\log(\tilde{m}_n(q,t)/q^n)$ order by order in $1/q$, in the same way as we did previously for $\log(\tilde{m}_n(q)/q^n)$. This also relies on the identification of the numbers $\bar{M}_n^{(n-k)}(n-2j)$ as polynomials of n, with special re-exponentiation properties, as discussed now.

For $k = 0$, the corresponding leading semi-meander has winding $w = n$, hence

$$\bar{M}_n^{(n)}(n-2j) = \delta_{j,0}\,. \tag{D.2}$$

For large n and finite $k \geqslant 1$, the winding of a semi-meander of order n with $n-k$ connected components may only take the values $(n-2k), (n-2k+2), \ldots, (n-2)$. Indeed, if C denotes the number of circles of such a semi-meander with winding $(n-2j)$, there are $(n-k-C)$ connected components which are not circles, hence which occupy two or more bridges. Therefore we have the following lower bound on the order of the semi-meander

$$n \geqslant C + 2(n-k-C) \Leftrightarrow C \geqslant n-2k \tag{D.3}$$

and therefore, as each circle contributes 1 to the total winding,

$$w \geqslant C \geqslant n-2k\,. \tag{D.4}$$

When $k = 1$, all the one-kidney perturbations (4.3) of the leading semi-meander have winding $w = (n-2)$, hence

$$\bar{M}_n^{(n-1)}(n-2) = n-1 \tag{D.5}$$

When $k = 2$, let us reexamine the various semi-meanders obtained in Fig. 14: the perturbations of Figs. $14c_{1,2}$ have winding $(n-4)$, whereas those of Figs. $14c_{3,4}$ have winding $(n-2)$. Hence we have

$$\begin{aligned} \bar{M}_n^{(n-2)}(n-4) &= \frac{n(n-3)}{2} + \delta_{n,2}\,, \\ \bar{M}_n^{(n-2)}(n-2) &= 2(n-2)\,. \end{aligned} \tag{D.6}$$

The correction is ad hoc to yield a zero answer when $n = 2$.

With a little more patience, the enumeration of the semi-meanders of order n with $(n-3)$ connected components and fixed winding yields

$$\begin{aligned} \bar{M}_n^{(n-3)}(n-6) &= \frac{n(n-1)(n-5)}{6} + 2\delta_{n,3} + 2\delta_{n,4}\,, \\ \bar{M}_n^{(n-3)}(n-4) &= 2(n^2-4n+1) + 4\delta_{n,3}\,, \\ \bar{M}_n^{(n-3)}(n-2) &= 2(n-3)\,. \end{aligned} \tag{D.7}$$

In general, the $\bar{M}_n^{(n-k)}(w)$ form a decomposition of the $\bar{M}_n^{(n-k)}$, in the sense that

$$\sum_w \bar{M}_n^{(n-k)}(w) = \bar{M}_n^{(n-k)} . \tag{D.8}$$

In a way similar to the $\bar{M}_n^{(n-k)}$, we expect the numbers $\bar{M}_n^{(n-k)}(n-2j)$ to be, for large enough n, some polynomials of n, whose coefficients depend only on j and k. For small n, some corrections have to be added to recover the actual numbers from their polynomial part. More precisely, one can show that

$$\bar{M}_n^{(n-k)}(n-2j) = p_j^{(k)}(n) + \sum_{m=0}^{j-2} \delta_{n,k+j-m-2}\, \eta_m^{(k,j)} \tag{D.9}$$

for $1 \leqslant j \leqslant k \leqslant n$, where $p_j^{(k)}(x)$ is a polynomial of degree j of x ($p_0^{(0)}(x) = 1$), whose coefficients depend on j and k, and the $\eta_m^{(j,k)}$ are non-negative integer corrections. In particular, according to (D.8), we must have

$$\sum_{j=1}^{k} p_j^{(k)}(x) = p_k(x) . \tag{D.10}$$

We have computed the polynomials $p_j^{(k)}(x)$ for $0 \leqslant j \leqslant k \leqslant 14$, by using exact enumeration data on the $\bar{M}_n^{(n-k)}(n-2j)$ for $0 \leqslant j \leqslant k \leqslant n \leqslant 24$, and the re-exponentiation trick described in Section 4.1. These lead to the large-n asymptotics of the partition function (D.1) in the large-q regime

$$\bar{m}_n(q,t) \sim \bar{c}(q,t)\, \frac{\bar{R}(q,t)^n}{n^{\gamma(q,t)}} \tag{D.11}$$

with $\gamma(q,t) = 0$ as before, and with the following large-q series expansions:

$$\begin{aligned}
\bar{R}(q,t) = q + t &+ \frac{2t}{q} + \frac{2t}{q^2} + \frac{2t}{q^3} + \frac{2t(t-1)^2}{q^4} + \frac{2t(t^2-4t+1)}{q^5} \\
&+ \frac{2t(3t^2-8t+1)}{q^6} + \frac{2t(4t^4-8t^3+9t^2-12t+1)}{q^7} \\
&+ \frac{2t(10t^4-26t^3+28t^2-18t+1)}{q^8} \\
&+ \frac{2t(6t^5+12t^4-61t^3+64t^2-24t+1)}{q^9} \\
&+ \frac{2t(24t^6-52t^5+71t^4-137t^3+131t^2-32t+1)}{q^{10}} \\
&+ \frac{2t(101t^6-260t^5+308t^4-324t^3+237t^2-40t+1)}{q^{11}} \\
&+ \frac{2t(90t^7+50t^6-610t^5+894t^4-726t^3+400t^2-50t+1)}{q^{12}}
\end{aligned}$$

$$+\frac{2t(173t^8-243t^7+409t^6-1507t^5+2237t^4-1564t^3+631t^2-60t+1)}{q^{13}}$$

$$+O\left(\frac{1}{q^{14}}\right), \tag{D.12}$$

$$\bar{c}(q,t)=1-\frac{t}{q}-\frac{4t}{q^2}+\frac{2t(t-3)}{q^3}+\frac{8t(t-1)}{q^4}-\frac{2t(7t^2-19t+5)}{q^5}$$
$$+\frac{2t(2t^3-13t^2+39t-6)}{q^6}+\frac{2t(18t^3-62t^2+79t-7)}{q^7}$$
$$-\frac{2t(45t^4-122t^3+183t^2-128t+8)}{q^8}$$
$$+\frac{2t(9t^5-138t^4+406t^3-514t^2+205t-9)}{q^9}$$
$$+\frac{2t(69t^5-475t^4+1138t^3-1143t^2+295t-10)}{q^{10}}$$
$$-\frac{2t(353t^6-1183t^5+2104t^4-3012t^3+2342t^2-421t+11)}{q^{11}}$$
$$+\frac{2t(56t^7-1553t^6+4986t^5-7692t^4+7668t^3-4311t^2+564t-12)}{q^{12}}$$
$$-\frac{2t(230t^7+3888t^6-14710t^5+22124t^4-17898t^3+7490t^2-751t+13)}{q^{13}}$$
$$-\frac{2t}{q^{14}}(3123t^8-10053t^7+22655t^6-45694t^5+58185t^4-39176t^3$$
$$+12215t^2-959t+14)+O\left(\frac{1}{q^{15}}\right). \tag{D.13}$$

The previous results (4.12) are recovered up to order 14 in $1/q$ by taking $t=1$. Let us look more closely at the expressions (D.12) and (D.13) above: we may Taylor-expand them as functions of t for small t. Remarkably, due to the structure of the coefficients of $p_j^{(k)}(x)$, which are themselves polynomials of k for fixed j (e.g. we have $p_1^{(k)}(x)=2(x-k)$ for all $k\geqslant 2$ while $p_1^{(1)}(x)=x-1$), we have been able to re-sum the large-q series coefficients of this expansion up to order 3 in t, in the following form:

$$\bar{R}(q,t)=q+t\frac{q+1}{q-1}-4t^2\frac{1}{(q-1)^2(q^2-1)}$$
$$+4t^3\frac{q^7-q^6+5q^4+11q^3+8q^2+q-1}{q^2(q-1)^2(q^2-1)^2(q^3-1)}+O(t^4),$$
$$\bar{c}(q,t)=1-t\frac{q^2+2q-1}{q(q-1)^2}+2t^2\frac{q^5+2q^4+10q^3+q^2-3q+1}{q^2(q-1)^2(q^2-1)^2}$$
$$-2\frac{t^3}{q^4(q-1)(q^2-1)^3(q^3-1)^2}(7q^{12}+6q^{11}+28q^{10}+89q^9+193q^8$$

$$+228q^7 + 147q^6 + 35q^5 - 14q^4 - 5q^3 + 6q^2 + q - 1) + O(t^4). \quad \text{(D.14)}$$

This structure is very reminiscent of the large-Q Q-state Potts model free energy [11], and suggests a possible expression in terms of modular forms of q.

The average winding in large-q semi-meanders is obtained by the formula

$$\langle w\rangle_n(q) = n - 2t\frac{d}{dt}\log \bar{m}_n(q,t)|_{t=1}\,, \quad \text{(D.15)}$$

leading to the expression (4.17) through the identifications

$$\lambda(q) = 1 - 2t\frac{d}{dt}\log \bar{R}(q,t)|_{t=1}\,,$$
$$\mu(q) = -2t\frac{d}{dt}\log \bar{c}(q,t)|_{t=1}\,. \quad \text{(D.16)}$$

Appendix E. Fine structure of the meander numbers

By simple inspection of the meander numbers (which we read from the semi-meander numbers with zero winding), we have found the following structure for the numbers $M_n^{(n-k)}$:

$$M_n^{(n-k)} = c_n r_k(n)\,, \quad \text{(E.1)}$$

where c_n is a Catalan number (2.4), $r_k(x)$ is a rational fraction of x with total degree k. More precisely, we have $r_0(n) = 1$ and for $k \geqslant 1$

$$r_k(n) = \frac{2^k n!(n+1)!}{k!(n-k-1)!(n+2k)!}\varphi_{2k-2}(n)$$
$$= \frac{2^k}{k!}\frac{n(n-1)(n-2)\ldots(n-k)}{(n+2)(n+3)\ldots(n+2k)}\varphi_{2k-2}(n)\,, \quad \text{(E.2)}$$

where $\varphi_{2k-2}(x)$ are monic polynomials of x of degree $(2k-2)$. They read, for $k = 1,2,\ldots,6$

$$\varphi_0(x) = 1\,,$$
$$\varphi_2(x) = x^2 + 7x - 2\,,$$
$$\varphi_4(x) = x^4 + 20x^3 + 107x^2 - 107x + 15\,,$$
$$\varphi_6(x) = x^6 + 39x^5 + 547x^4 + 2565x^3 - 5474x^2 + 2382x - 672\,,$$
$$\varphi_8(x) = x^8 + 64x^7 + 1646x^6 + 20074x^5 + 83669x^4 - 323444x^3$$
$$+257134x^2 - 155604x + 45360$$
$$\varphi_{10}(x) = x^{10} + 95x^9 + 3840x^8 + 83070x^7 + 940443x^6 + 3382455x^5$$
$$-22294735x^4 + 27662860x^3 - 26147139x^2 + 16354530x - 4098600\,. \quad \text{(E.3)}$$

References

[1] K. Hoffman, K. Mehlhorn, P. Rosenstiehl and R. Tarjan, Sorting Jordan sequences in linear time using level-linked search trees, Information and Control 68 (1986) 170.

[2] V. Arnold, The branched covering of $CP_2 \to S_4$, hyperbolicity and projective topology, Siberian Math. J. 29 (1988) 717.

[3] K.H. Ko, L. Smolinsky, A combinatorial matrix in 3-manifold theory, Pacific. J. Math. 149 (1991) 319.

[4] J. Touchard, Contributions à l'étude du problème des timbres poste, Canad. J. Math. 2 (1950) 385.

[5] W. Lunnon, A map-folding problem, Math. of Computation 22 (1968) 193.

[6] S. Lando and A. Zvonkin, Plane and Projective Meanders, Theor. Comp. Sci. 117 (1993) 227; Meanders, Selecta Math. Sov. 11 (1992) 117.

[7] P. Di Francesco, O. Golinelli and E. Guitter, Meander, folding and arch statistics, *in* Special Issue: Combinatorics and Physics, Mathematical and Computer Modelling 144 (1996).

[8] Y. Makeenko, Strings, Matrix Models and Meanders, Proceedings of the 29th Inter. Ahrenshoop Symp., Germany (1995);
Y. Makeenko and H. Win Pe, Supersymmetric matrix models and the meander problem, preprint ITEP-TH-13/95 (1996);
G. Semenoff and R. Szabo, Fermionic Matrix Models, preprint UBC/*S*96/2 (1996).

[9] P. Di Francesco, O. Golinelli and E. Guitter, Meanders and the Temperley–Lieb algebra, Saclay preprint T96/008 (1996).

[10] N. Sloane, The on-line encyclopedia of integer sequences, E-mail: sequences@research.att.com.

[11] R. Baxter, Exactly solved models in statistical mechanics (Academic Press, London, 1982).